CLEEN
Cluster for Energy and Environment

CCSP WP5.2.2, D548
Turku 2015

Rickard Erlund
Evelina Koivisto
Hannu-Petteri Mattila
Ron Zevenhoven
Mats Fagerholm

Process for upgrading diopside-based rock for lime kiln gas CO_2 carbonation

CLEEN
Cluster for Energy and Environment

CLEEN LTD
ETELÄRANTA 10
P.O. BOX 10
FI-00130 HELSINKI
FINLAND
www.cleen.fi

ccsp
Carbon Capture and Storage Program

Åbo Akademi University
Nordkalk Oy Ab
CCSP WP5.2.2, D548

Rickard Erlund
Evelina Koivisto
Hannu-Petteri Mattila
Ron Zevenhoven
Mats Fagerholm

Process for upgrading diopside-based rock for lime kiln gas CO_2 carbonation

ccsp
Carbon Capture and Storage Program

Åbo Akademi University
Nordkalk Oy Ab
Turku/Parainen
August 2015

Report Title: Process for upgrading diopside-based rock for lime kiln gas CO_2 carbonation

Key words: mineral carbonation, silicate raw materials

Abstract:

As a follow-up of deliverable D513 (*Investigation of alternative-silicate raw materials for carbonation)* this report addresses the possibilities of upgrading diopside containing wall rock from a limestone quarry. The aim is to obtain magnesium (optionally also calcium and/or iron)-containing fractions that are suitable for large-scale CO_2 mineral sequestration.

An energy efficient option (ÅA route) for carbon capture and storage by mineralization is being developed at Åbo Akademi University. Previously, serpentinite has been successfully used in a multi-step process with the aim to convert magnesium silicate rock into hydroxides followed by carbonation. According to literature sources, it should be possible to convert diopside into serpentine under acidic conditions.

The material used in this study was concentrated ("enriched") by density separation, giving a dense diopside-rich fraction (ρ>3.3 kg/dm^3) and a lighter fraction (ρ<3.3 kg/dm^3). Both the dense fraction and the un-concentrated wall rock were tested with the aim to extract as much magnesium, calcium and iron as possible. The fractions were also pre-heated in a furnace to 1040 ºC in order to study if this thermal treatment would make the material more reactive.

Studies with Finnish serpentinite rock from Hitura nickel mine have shown promising extraction results and the method appears to be suitable for CO_2 sequestration. The theoretical capacity of sequestering CO_2 looks promising comparing the diopside-rich fraction of the wall rock with the Finnish serpentinite.

The experiments were made either as a chemical liquid/solid or thermal/chemical solid/solid test. The solid/liquid tests were performed with several different acids and also with/without presence of carbon dioxide. Phase separation after the extraction tests was performed in an inclined settler, resulting in up to four different fractions. The extraction step of the earlier developed ÅA route was also tested directly on both the concentrated as well as the un-concentrated wall rock, instead of serpentinite.

One important finding was that the concentrated diopside fraction showed a large substitution of magnesium by iron as hedenbergite, explaining also the significant iron oxides content of ~ 15 %-wt.

The highest obtained magnesium extraction from the diopside-rich fraction was 3.6 %-wt. Calcium and iron extractions reached almost 7 %-wt. and 5 %-wt.,

respectively.

The diopside rich wall rock from Parainen seems to be significantly less reactive than diopside (which is a pyroxene mineral) reported in literature. No conversion of diopside to serpentine was achieved in any of the experiments. These factors, together with the fact that a pre-concentration step still has to be added, make the wall rock unsuitable and un-attractive from an economical point of view to be used as a source of magnesium or calcium in the developed mineral carbonation processes.

Table of contents

1 Introduction

Mineral carbonation of magnesium rich silicate minerals such as serpentinite ($Mg_3Si_2O_5(OH)_4$) using the so-called ÅA route (Figure 1) has been discussed in e.g. previous research reports D503, D504 and D510[1]. In addition, D513 presented a preliminary comparison of alternative silicate raw materials for the process based on solid/solid reaction of the Mg-carrier and ammonium sulfate (AS, $(NH_4)_2SO_4$). Because the target of this research work is to develop a mineral carbonation – based carbon capture and storage (CCS) method for an industrial lime kiln and the kiln is located near a limestone quarry rich in diopside ($MgCaSi_2O_6$), a possibility to utilize this material instead of serpentinite has been studied in detail.

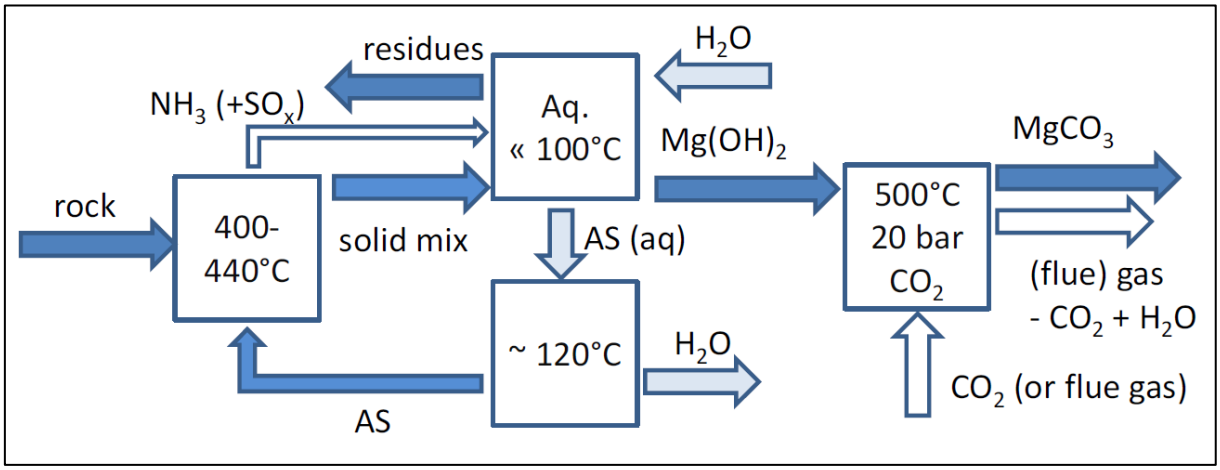

Figure 1. A schematic illustration of the ÅA mineral carbonation process with gas-solid carbonation. AS: ammonium sulfate (D513)

Several methods to increase the reactivity of magnesium or calcium in the diopside mineral, i.e. to produce dissolved Mg/Ca ions or reactive solids, have been tested, as suggested in the literature and based on earlier experience at ÅA. These methods comprise of both chemical aqueous/solid (e.g. acid and ammonium salt) and chemical/thermal solid/solid treatments, as discussed below.

Diopside belongs to the pyroxene group with silicon-oxygen tetrahedral chains. In the diopside rich fraction - obtained after pre-concentration of the wall rock from the limestone quarry - approximately half of the magnesium is substituted by iron. Thus, twice the amount of diopside would be required for the same amount of magnesium extraction compared to a more Mg-rich material. The pure pyroxene with magnesium substituted by iron is called hedenbergite and the Mg-Fe substitution giving the diopside-hedenbergite series also results in minor changes in the Si-O chain configuration, (Deer et al., 1992).

[1] Note that an alternative ÅA route involves carbonation of $MgSO_4$ in an aqueous solution, (Zevenhoven et al., 2015).

The chemical reaction transferring diopside into serpentine under acidic conditions in aqueous solutions is shown in reaction R1 suggested in the literature (Lu et al., 2011, Frost and Beard, 2007) – this was a starting point for this study. Simultaneously, large amounts of calcium and silica would be released, as dissolved ions and as a solid fraction, respectively. Besides Mg, also Ca may eventually be carbonated. Based on stoichiometry, diopside releases three moles Ca for each mole serpentine formed. The extraction rate of calcium can thus be seen as an indicator of the rate and extent of R1. This reaction occurs slowly also under neutral pH conditions,

$$3\,CaMgSi_2O_6 + 6\,H^+ \rightarrow Mg_3Si_2O_5(OH)_4 + 3\,Ca^{2+} + H_2O + 4\,SiO_2 \qquad \text{(R1)}$$

diopside serpentine

Figure A-1 in Appendix A shows also the reactivity of diopside to a more reactive sepiolite ($Mg_4Si_6O_{15}(OH)_2 \cdot 6H_2O$) under acidic conditions in an equilibrium diagram.

A theoretical comparison of the concentrated diopside-rich fraction of the wall rock with serpentinite from Hitura, suggests that diopside could in principle suit for mineral carbonation as well (Figure 2-Figure 4). The total amount of elements that possibly could bind CO_2 is slightly above 30 %-wt. for both the diopside-rich fraction and serpentinite from the Hitura nickel mine (Figure 2).

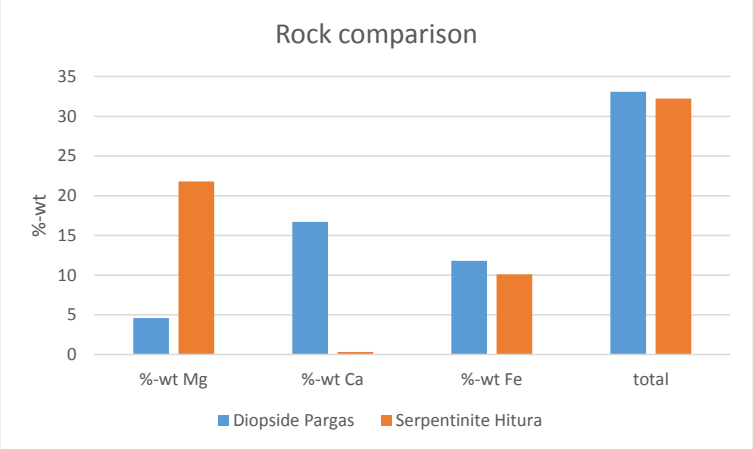

Figure 2. Rock composition of serpentinite from Hitura and the diopside-rich fraction from the wall rock of a limestone quarry. Ca, Fe and Mg are compared and a total share of the three elements for the two rocks, respectively, are compared in the bars to the right.

The binding capacity as amount CO_2/ tonne rock is in the same range for both rocks, for the serpentinite from the Hitura nickel mine 480 kg CO_2/tonne rock and for the diopside-rich fraction 350 kg CO_2/tonne rock (Figure 3).

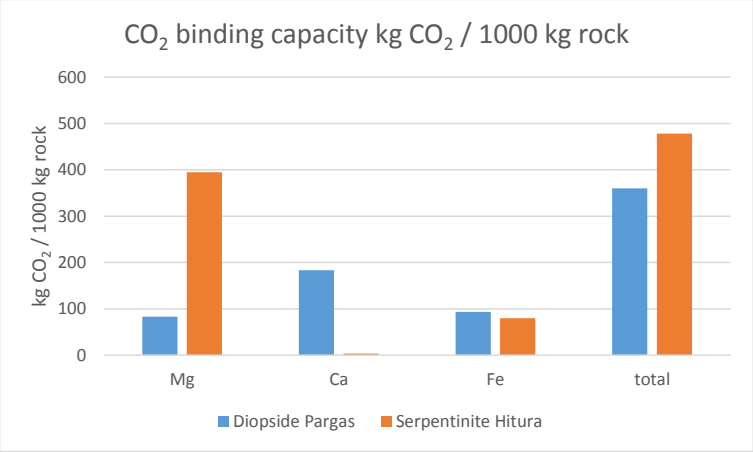

Figure 3. CO_2 binding capacity in kg CO_2/ tonne rock. Comparison of Ca, Fe and Mg and a total binding capacity for Hitura serpentinite and the diopside-rich fraction from the wall rock of a limestone quarry.

The amount rock needed to sequester one tonne of CO_2 is almost 4 tonnes of diopside-rich fraction of the wall rock and 2.5 tonnes of serpentinite from Hitura nickel mine, assuming that only Ca and Mg would contribute to the carbonation. Fe could possibly be better used in iron and steelmaking (Romaõ et al., 2012, Koivisto, 2013). The binding capacity of CO_2 for Ca in the serpentinite rock is much lower than the other elements in the diagram in Figure 4. The reason is that the serpentinite is very low in calcium, so large amounts of rock would be needed if only Ca in the rock would bind CO_2. The combined binding capacities of Mg+Ca and Mg+Ca+Fe are given in Figure 4 as well.

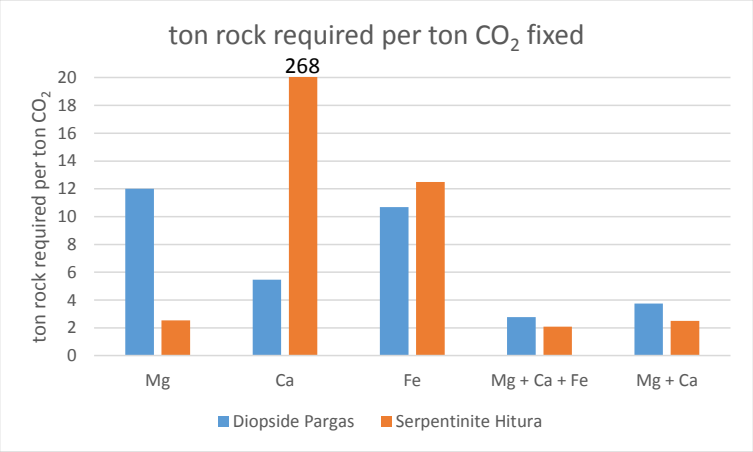

Figure 4. Tonne rock required per tonne of CO_2 fixed. Comparison of Ca, Fe and Mg given separately and together for serpentinite from the Hitura nickel mine and the diopside-rich fraction from the wall rock of a limestone quarry, respectively.

However, some authors (Sanna et al., 2014) state that pyroxenes are chemically quite stable. Experimental results with a diopside-containing pyroxene reacting with aqueous ammonium bisulphate (ABS, NH_4HSO_4) resulted into a Mg-extraction of only 30% after 3h, while a 70% Mg-extraction was obtained using olivine ($(Mg,Fe)_2SiO_4$) rock, (Sanna et al., 2014). Also, from lizardite-type serpentinite more

than 85% of the magnesium was extracted after 3h. Interestingly, two thirds of the magnesium was already extracted after approximately 5 minutes, (Styles et al., 2014).

Various input minerals for the ÅA route (Figure 1) were earlier analyzed by Sjöblom and Eklund (2014), concluding that only minerals with 17-27 %-wt. Mg and >2.5 %-wt. crystal water released Mg efficiently (>40 %-wt.). It seems that the single tetrahedral silica chain in pyroxenes causes these minerals to be less eager to dissolve whereas the crystal water of e.g. serpentine introduces more chemical instability into the structure, (Sjöblom and Eklund, 2014). Figure 5 shows differences in the structure of diopside and serpentine. Equilibrium diagrams obtained with HSC 8.0 also show that diopside is more stable than serpentinite at temperatures below 1000 °C (Appendix B).

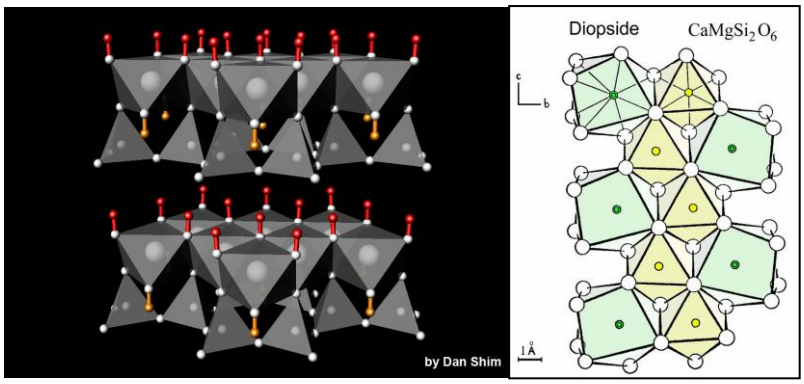

Figure 5. Structure of serpentine (left, Arizona State University) and diopside (right, California Institute of Technology).

Figure 6 shows the structure of a pyroxene sample. The shape of the pyroxene grains will remain even if conversion of pyroxene to serpentine will take place. This could also make minerals originating from pyroxene being less reactive.

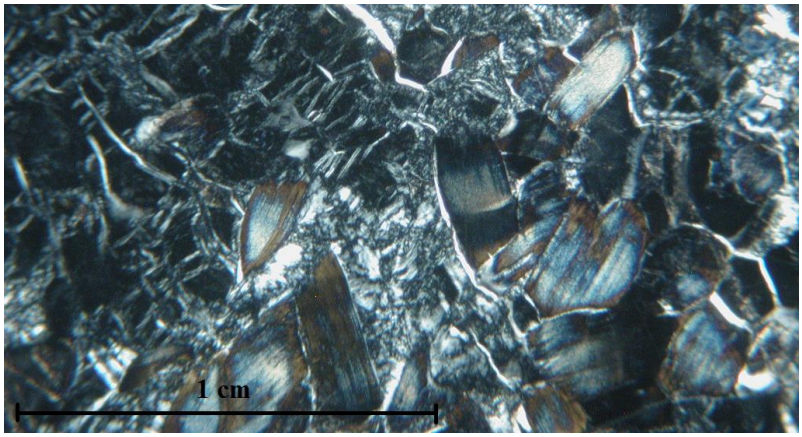

Figure 6. Microscopic image of a pyroxene sample. The blue-brownish grains are bastite grains which are formed along pyroxene edges as they convert to serpentinite. The structure of pyroxene will remain and the structure will remain even if bastite starts to decompose. (Published and modified with permission from Sjöblom, S., Åbo Akademi University 2015)

2 Materials and methods

2.1. Materials

Table 1 represents the chemical composition of serpentinite overburden rock from the Hitura nickel mine (D510), as well as specified fractions of un-concentrated "as delivered" and concentrated diopside rock from Parainen limestone quarry, based on XRF analysis. The diopside concentration was performed by the Geological Survey of Finland (GTK) based on density separation by means of heavy liquids. The concentrated, diopside-rich fraction, has a density below 3300 kg/m^3. Particle size fractions used in this study were 63-125 µm and 125-250 µm.

As can be seen from Table 1, the diopside material contains much less magnesium compared to the serpentinite, even after the enrichment procedure. On the other hand, the calcium content is much higher in the diopside material. Before concentration, alumina content is high in the diopside rich rock, but the concentrated fraction actually contains more iron.

Table 1. Chemical compositions of various serpentinite and diopside fractions, based on XRF analysis. X= not analyzed by XRF. (Analysis of serpentinite from Nduagu et al., 2012, diopside analyses by Nordkalk, Parainen, Finland)

Compound	Unit	Serpentinite	Diopside		
			Unconcentrated	Concentrated	
		75-125 µm	125-250 µm	63-125 µm	125-250 µm
CaO	%-wt.	0.5	17.0	22.4	23.4
SiO_2	%-wt.	24.8	52.3	49.7	49.2
TiO_2	%-wt.	-	0.3	1.6	0.7
Al_2O_3	%-wt.	0.1	14.7	3.3	1.6
Fe_2O_3	%-wt.	14.4	4.6	14.8	16.9
MgO	%-wt.	36.2	2.0	6.3	7.6
K_2O	%-wt.	-	3.6	0.32	0.1
Na_2O	%-wt.	-	1.5	0.31	0.2
MnO	%-wt.	-	<0.1	0.24	0.3
P_2O_5	%-wt.	-	<0.1	0.17	<0.1
Rest	%-wt.	24.1	<4.0	<1.0	<0.1
Analysis number			57577	57396	57338

Table 2. Mineralogy of the various serpentinite and diopside fractions. Estimated on basis of XRD analysis and the chemical composition.

Compound	Serpentinite (%-wt.)	Diopside (%-wt.)	
		Unconcentrated	Concentrated
Diopside-Hedenbergite	-	20-25	90-95
Plagioclase $(Na,Ca)(Si,Al)_4O_8$	-	30-35	< 5
Feldspar $KAlSi_3O_8 – NaAlSi_3O_8 –CaAl_2Si_2O_8$	-	20-25	-
Quartz SiO_2	-	5-10	-
Wollastonite $CaSiO_3$	-	5-10	-
Calcite $CaCO_3$	-	5-10	-
Epidote $Ca_2(Fe,Al)Al_2(SiO_4)(Si_2O_7)O(OH)$	-	< 5	-
Cordierite $Mg_2Al_4Si_5O_{18}$	-	-	< 5
Serpentine $(Mg, Fe)_3Si_2O_5(OH)_4$	83	-	-
Magnetite Fe_3O_4	14	-	-
Rest	3	-	-

The unconcentrated as well as the concentrated fraction of the wall rock were also heated to 1040 ºC for 30 minutes in order to see if thermal pre-treatment would make the rock more reactive. The idea was to see if it could be possible to “shatter” the silica structure by this treatment, thereby achieving better extraction of calcium and magnesium. A few tests were made with burnt rock. Figure 7 shows the color differences between the different fractions and between thermally treated and untreated fractions.

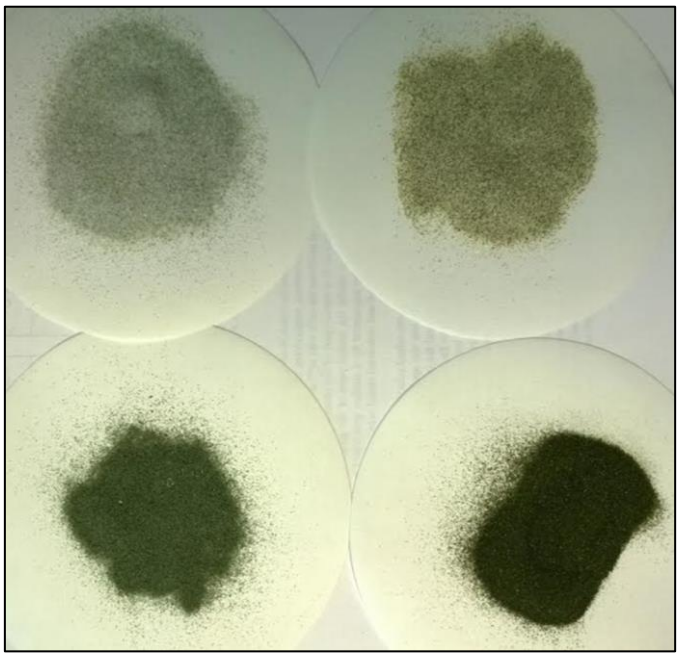

Figure 7. Photo of the different materials used. Upper left: Unburnt, unconcentrated wall rock, Upper right: Burnt, unconcentrated wall rock, Lower left: Unburnt, concentrated diopside rich wall rock, Lower right: Burnt, concentrated diopside rich wall rock

2.2. Methods

The goal of this study was to see whether the diopside could be converted into serpentine, which then could be used as feed in the ÅA route. Different lixiviants were tested in order to achieve an efficient conversion and the diopside-rich rock was also directly used as feed to the ÅA route.

All methods used are based either on aqueous leaching steps or on solid /solid thermal reactions, which in the following sections will be presented separately. The parameters and results will be presented more in detail together with the results because the parameters vary from test to test.

3 Experimental work with diopside

As mentioned above, based on the open literature and previous work with serpentinite and calcium silicates (e.g. D527, D528, D532), several experimental attempts were made to efficiently extract magnesium and/or calcium from the diopside material. Table 3 and Table 4 list the applied aqueous and solid/solid methods, together with the limits of the various experimental parameters.

Table 3. The applied Mg/Ca leaching/extraction methods for diopside rock by aqueous process routes.

Chemical lixiviant	Conc. (M)	Solution pH	Time (h)	Temperature (°C)
NH_4Cl	0.1-2.0	5.00	5-20	20-50
$NH_4Cl + CO_2$	0.1-2.0	4.00	5-20	20-50
NH_4HSO_4	0.1-0.2	1.00	3-20	20
$(NH_4)_2SO_4$	0.2-1.4	4.00	20	20-70
Acetic acid	3.5-17.5	1.75-3.00	1-20	20-60
Citric Acid	0.5	1.65	5	20
Oxalic Acid	0.5	1.26	5	20
Formic Acid	0.5	2.08	5	20
HCl	0.5	0.30	5	20-50
$HCl + NH_4Cl$	0.1-0.5	0.30	5-24	20-50
HNO_3	0.15	1.00	5	20

Table 4. The applied Mg/Ca extraction parameters for diopside rock by thermal solid/solid process routes. Tests marked with * were run in a chamber furnace, while the others were run in a rotary kiln. D=diopside, 63-125, 125-250=particle size in µm, UC=un-concentrated, B=burnt. H_2O_{tot} is total amount of water added for cooling and in experiments under 90 °C also H_2O added as reactant.

Mineral	Mineral (g)	Reagent	Reagent (g)	Temp (°C)	Time (min)	H_2O_{tot} (ml)
D, 125-250	40.00	AS	50.00	440	60	500
*, D, 63-150	25.00	ABS	25.00	440	60	315+2
*, D, 63-150	25.00	ABS	25.00	440	60	315
D, 125-250	40.00	ABS	40.00	90	180	515
*, Fraction 2 (no 73)	1.00	ABS	1.00	480	60	40
*, Fraction 2 (no 73)	1.00	AS	1.25	480	60	40
D , B, UC, 125-250	40.00	AS	50.00	440	60	500
D, B, 125-250	30.00	ABS	30.00	90	240	390
D, B, 125-250	30.00	ABS	30.00	440	60	375
D, UC, 125-250	30.00	ABS	40.00	440	60	375

3.1 One-step aqueous leaching with acids

The first series of tests was done with 5 grams of diopside and an aqueous solution volume between 20 and 100 mL, using different acids and concentrations in a magnetically stirred vessel. The reaction time, particle size and temperature were also varied to monitor the effects to the leaching performance. The tests showed that the leaching reaction is kinetically very slow as is seen from the results presented in Table 5. The best result obtained regarding Ca^{2+} extraction was ~1 % of total Ca present in the mineral (Test 81). X-Ray Diffraction analysis confirmed that no substances as suggested in reaction R1 were produced during the experiments (Appendix C). Also, the extraction efficiency of other elements remained low.

Earlier experiments using a diopside sample from the same limestone quarry had shown a Ca^{2+} extraction efficiency as high as 10.7% (Test 1 in Table 5, also D513), though this sample had not been concentrated as some of the material used here. As it is known that the dissolution of limestone (calcite, $CaCO_3$) is fast under acidic conditions, the calcium may have been extracted from limestone, also releasing CO_2 which makes it unsuitable as a raw material for mineral carbonation based CCS processes.

Table 5. Calcium, magnesium and iron extraction results from aqueous acid leaching experiments. (Acetic, hydrochloric, oxalic and formic acid) Experiment 1 is a reference test with un-concentrated diopside rock as discussed earlier in D513.

#	Mass stone (g)	Reaction time (h)	Extraction (%-wt.) Ca^{2+}	Mg^{2+}	$Fe^{2/3+}$	c_{Acid} (M)	Acid	pH start	Temp. (°C)
1	20	3	10.7	-	-	17.50	HAc	1.76	20
8	5	3	0.13	0.31	0.07	17.50	HAc	1.76	20
18	5	1	0.02	0.11	0.10	17.50	HAc	1.76	20
20	5	3	0.05	0.08	0.02	1.75	HAc	2.26	40
21	5	6	0.12	0.44	0.04	1.75	HAc	2.26	40
22	5	3	0.73	0.37	0.08	3.50	HAc	2.11	40
26	5	3	0.04	0.48	0.02	17.50	HAc	1.76	40
30	5	3	0.22	1.42	0.02	17.50	HAc	1.76	20
32	5	3	0.90	0.37	0.20	0.15	HCl	0.83-2.0	20
80	10	5	0.32	0.90	0.89	0.50	OxAc	1.26	20
81	10	5	1.29	1.63	1.37	0.50	HCOOH	2.08	20
82	10	5	0.73	0.23	0.30	0.50	CitrAc	1.65	20

The last experiments with oxalic, formic and citric acid did not show any increased extraction of calcium, magnesium and iron compared to earlier tests (Table 5).

3.2 Multi-step aqueous leaching and size classification

3.2.1 Ammonium salts

Earlier studies (e.g. D532) have shown that aqueous ammonium salt solutions are able to lixiviate (leach) calcium from certain calcium silicates such as larnite (Ca_2SiO_4). Also, near-neutral pH conditions are in that case favorable regarding both calcium release and carbonation of the aqueous ions, because the process can be operated on pH-swing basis, i.e. without addition of acids or bases between the reaction steps.

The suitability of similar methods for Ca/Mg leaching and carbonation based on diopside was tested with ammonium acetate, ammonium nitrate, ammonium chloride and ammonium sulfate. However, the leaching efficiency of calcium still remained below 1%-wt., being similar to the results obtained with acids. During the reaction, the particle size distribution (PSD) of the diopside material decreased, which was primarily observed from formation of fluidized particles in the solution. It seems that the minor Ca leaching effect combined with less acidic pH conditions and mixing was largely grinding the diopside particles into smaller sizes. Considering this effect, the most efficient of the ammonium salts was ammonium chloride, as discussed below.

3.2.2 Size classification using an inclined settler

An inclined settler is a relatively simple device capable of efficiently separating solids with different settling properties, as described in e.g. D532. In this study, the diopside material treated with ammonium salt solutions, was (after a reaction time of 5-20 h) pumped through an inclined settler with a diameter of 5 cm, length of 50 cm, inclination of 45° and a circular cross-section (Figure 8).

The reacted diopside particles were classified into three major fractions (F2-F4) using the settler. F3 and F4 were separated in an additional mixing stage in the reaction vessel, where the re-fluidized fraction formed the F3 material. Differences in particle size of the different fractions are found in Figure 9. F1 only formed a minor fraction, though it was analyzed separately using XRF/XRD analysis. Figure 10 represents the formation of fractions F2 and F3 in a series of experiments. In general it can be seen that a longer reaction time (20 h vs. 5 h) favors formation of F2 and F3 fractions.

Figure 11 shows the comparison of the F4 PSD (Tests 64, 65) with the starting material. Fractions F1-F3 consisted only of particles smaller than 38µm (which was the smallest sieve available) and thus not included in Figure 11. Both tests were performed using the same reaction conditions, thus representing the high variation in the obtained PSD.

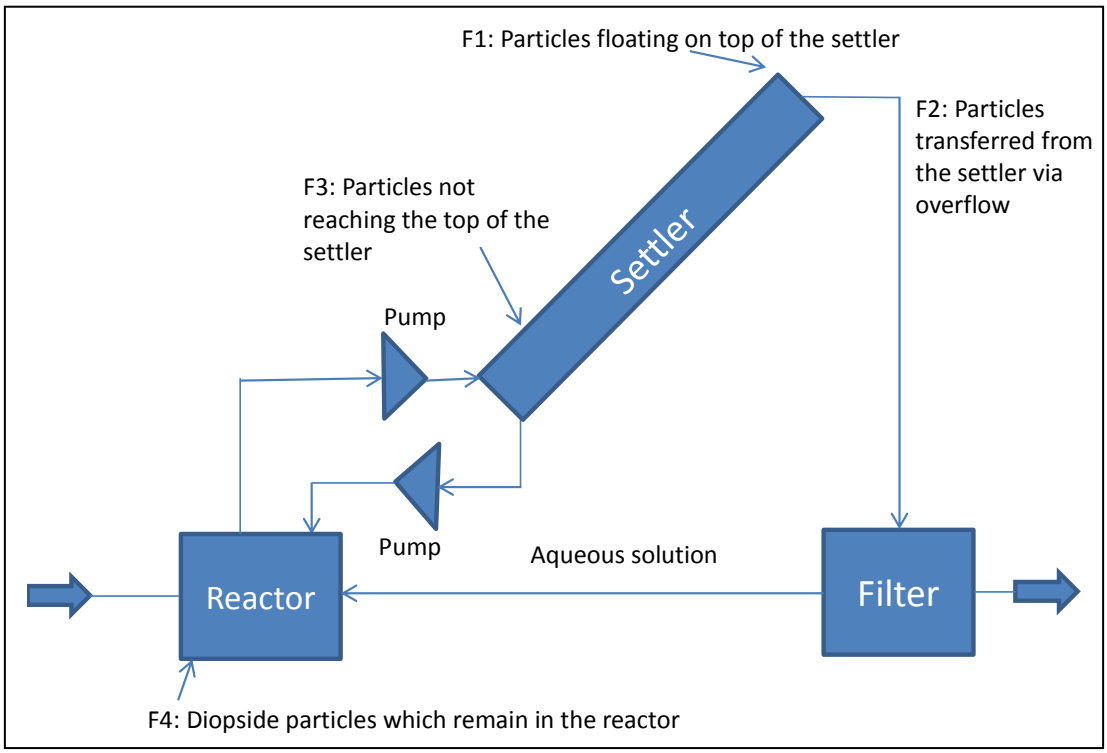

Figure 8. The inclined settler used as a size classifier for the diopside material

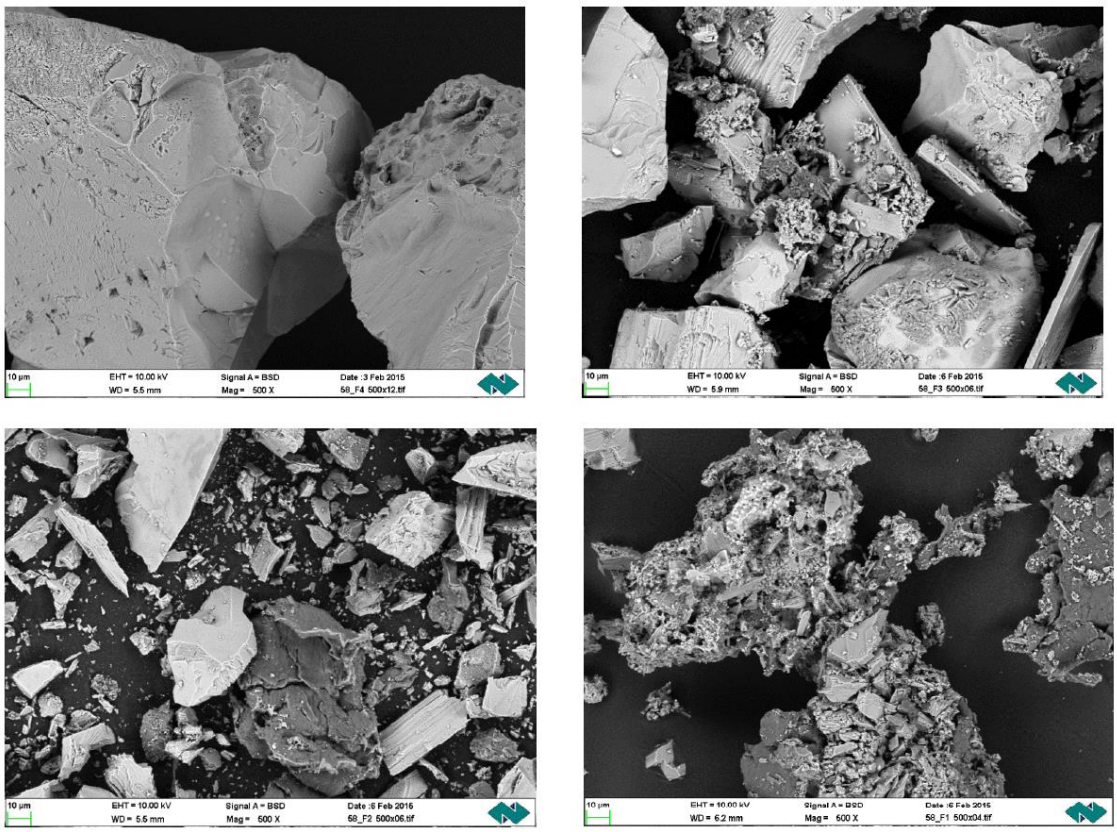

Figure 9. SEM-pictures of the fractions after experiment 58. Pictures on the upper row show F4 (left) and F3 (right). On the lower row F2 (left) and F1 (right) are shown.

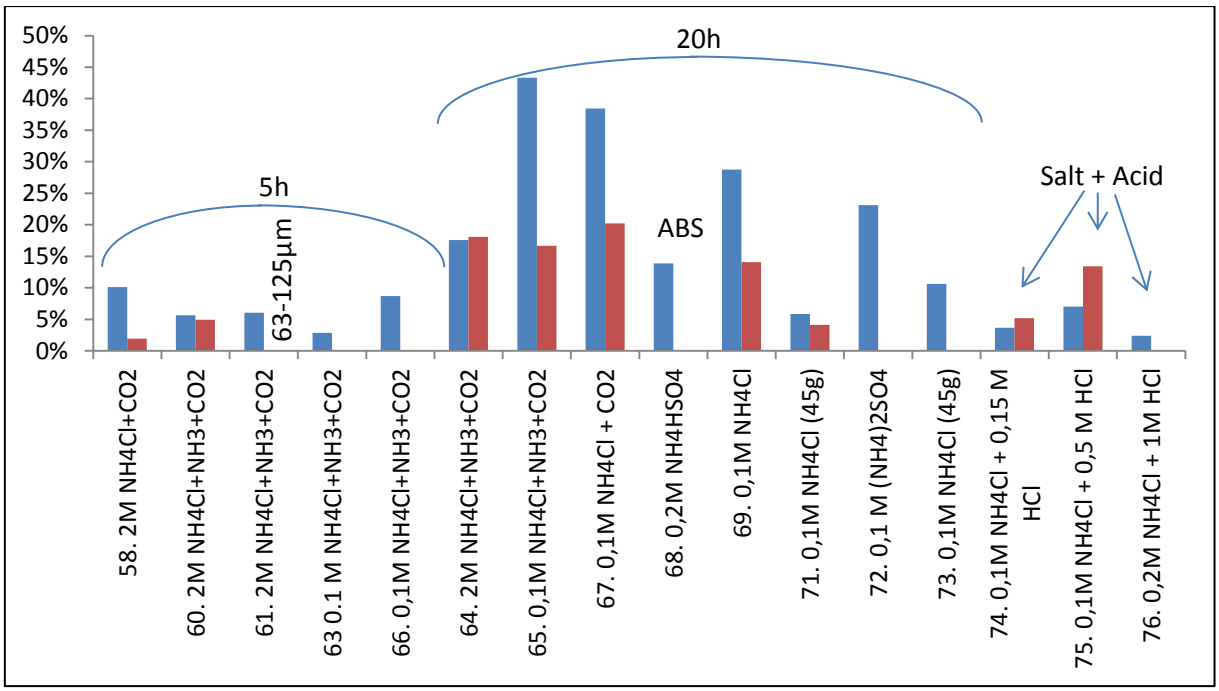

Figure 10. Mass fractions F2 (blue) and F3 (red), %-wt. for several experiments.

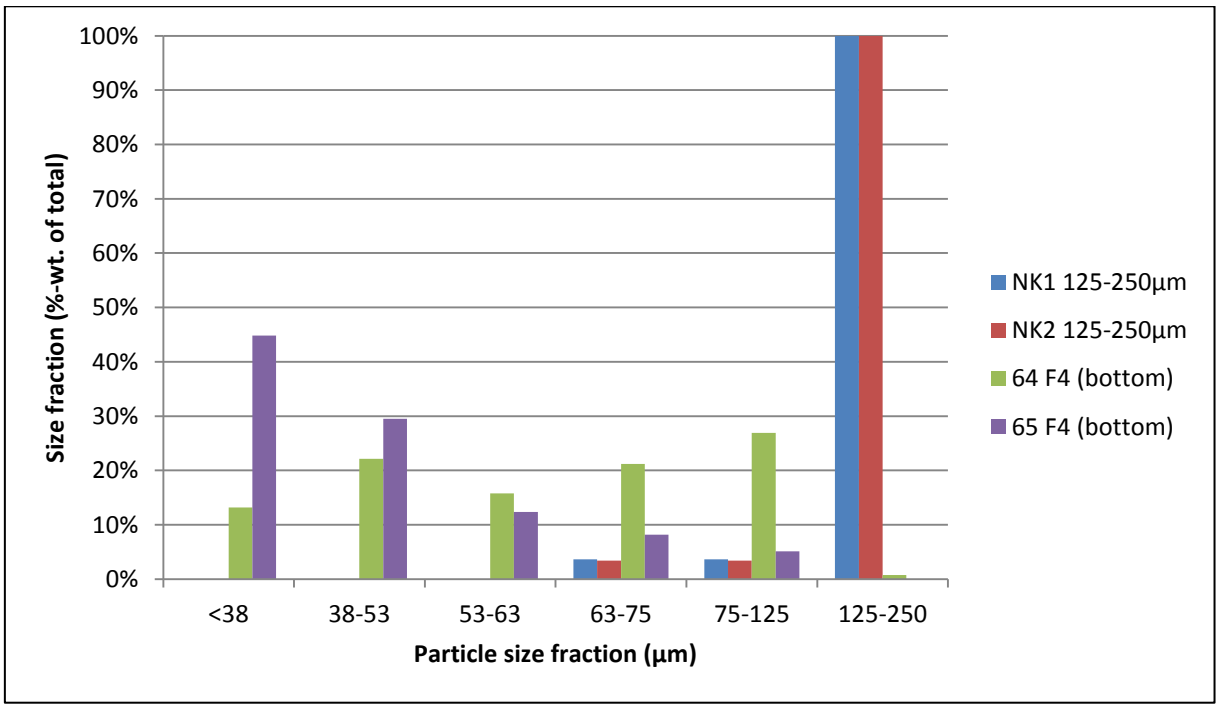

Figure 11. Particle size distribution of the original diopside samples (NK1, NK2 125-250 µm) together with PSD for F4 fraction from experiments 64 and 65.

3.2.3 Chemical changes during ammonium salt leaching

Despite of the changes in PSD as described above, all the fractions F1-F4 consisted mainly of diopside according to XRD analyses (Figure C-2, Appendix C). However, all the fractions also had a somewhat lower Ca content than the diopside starting material. Fraction F2 showed a significant loss on ignition (LOI) at 550°C (Appendix D). The XRD results showed an amorphous peak at 2Θ=21°(Co) for the reaction products, especially for the lighter fractions (Figure C-2, Appendix C). This peak seems to correspond to the signal of calcium hydroxide, indicating that some of the calcium present in diopside would have been hydrated, although not dissolved from the solids, during the reaction**.**

It has been reported also in the literature that calcium and magnesium on the mineral surface can bind directly to hydroxide (Peck et al., 1998). Calculating for sample 50 with the highest LOI (550°C) value, if all Ca and Mg would be hydrated, a similar LOI value would be reached. However, compared to a synthetic diopside used in the literature (Peck et al., 1988), the iron-rich material used here would give a possibility also for hydration of iron, besides Ca and Mg. The results indicate that only calcium and possibly magnesium are hydrated.

Table 6. Loss-on-ignition of samples from different experiments using concentrated diopside. Also the theoretical estimates for LOI in experiment 50 with hydrated Ca, Ca and Mg and Ca, Mg and Fe are shown for comparison.

Experiment	Lixiviant	Concentration (M)	LOI (%)	pH
50, hydrated Ca			14.2	
50, hydrated Ca, Mg			20.6	
50, hydrated Ca, Mg, Fe			27.8	
50	NH_4Cl	0.2	20.1	6.0
58	NH_4Cl	2	13.9	4.5
60	$NH_4Cl/NH_3 + CO_2$	2/0.8	5.4	7.5

3.2.4 Direct aqueous carbonation of hydrated diopside

The hydrated F2 fraction possibly containing calcium hydroxide could be interesting for direct carbonation tests. For this, the solid hydrated mineral was added in an alkaline aqueous solution with 0.5M NH_3, and a CO_2 gas stream was bubbled through the solution. This was done to maintain a pH value above 7, thus enabling the possibility of calcium carbonate precipitation. Figure 12 presents the experimental carbonation efficiencies measured using the gasometric carbonate content analysis developed at ÅA, (Fagerlund et al., 2010).

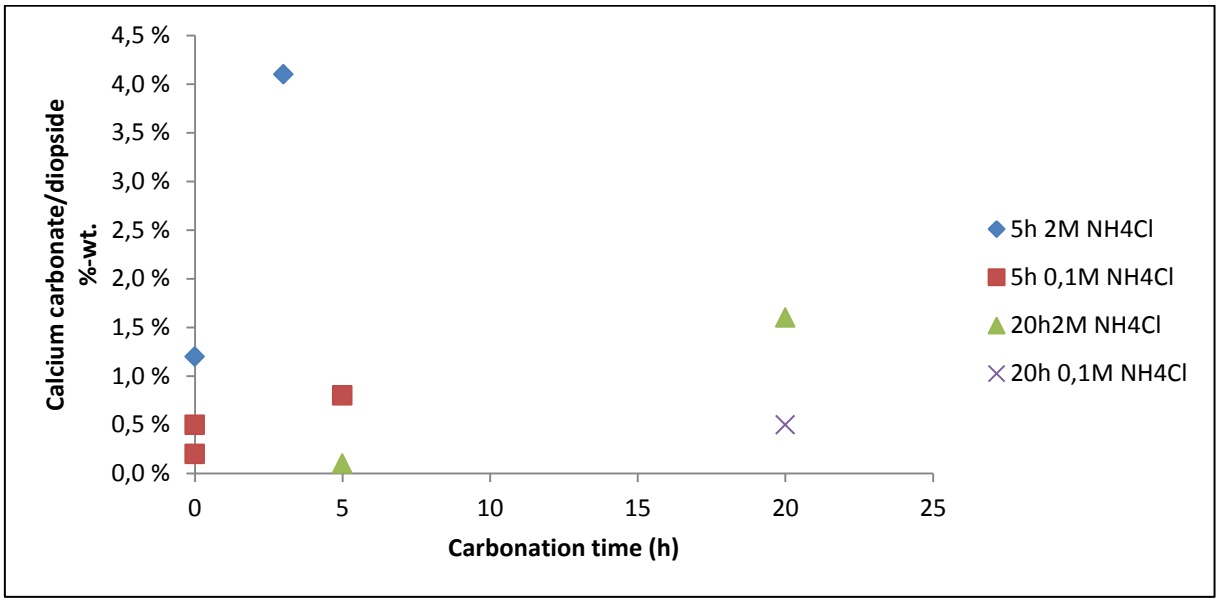

Figure 12. Calcium carbonate contents in the carbonated samples of F2. Theoretical maximum value is 28%.

Even though theoretically 28%-wt. of the sample could consist of calcium carbonate, only values below 5%-wt. were obtained. The results show that only a part of the calcium hydroxide can be carbonated using the direct aqueous carbonation approach for the hydrated F2 fraction. It seems that only the completely dissolved calcium ions carbonate efficiently, the reason being that carbonate ions, unlike hydroxide, are divalent, which means that carbonate ions only will bind efficiently to free Ca^{2+} in the solution, Figure 13, (Metafysica, 2015).

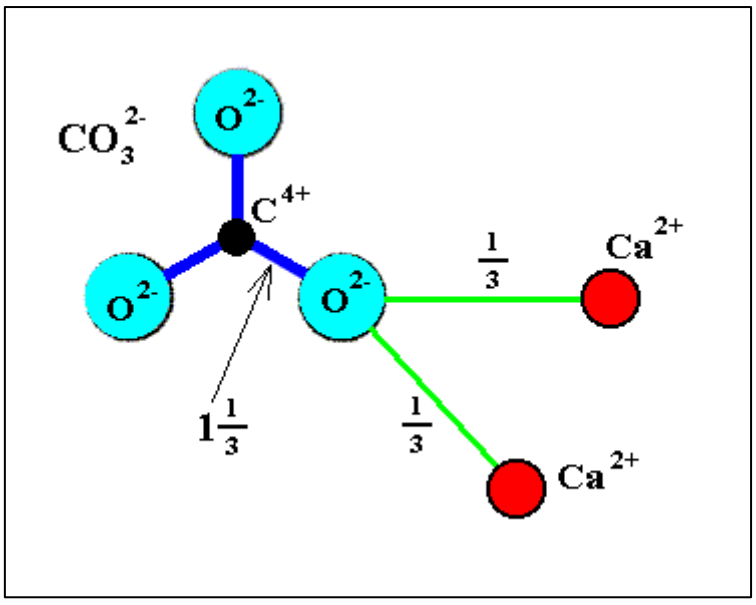

Figure 13. Possibilities for Ca^{2+} ion to bind to CO^{2-}_3 ions (Metafysica, 2015).

3.2.5 **Acid leaching with size classification and separation of fines**

As discussed above, the ammonium salt experiments with the size classification had a strong impact on the solids particle size, which decreased for all fractions. It was hypothesized that a consequent acid leaching might increase the extraction efficiency of the target metals, i.e. Ca and Mg, because the smaller particle size and continuous grinding would eventually cause the silica bonds to break, (Peck et al., 1998). Also, the smaller particle size would give a larger specific surface area between the particle and the solution.

To study this assumption, a two-step test was performed as follows: firstly, diopside (125-250µm) was leached in 0.5l of 0.1M NH_4Cl for 20 hours, after which the F2 fraction was separated using an inclined settler as described above. Secondly, the F2 fraction was leached in a 0.5l of 0.15M HCl solution for 5 hours. The results were clear: the calcium extraction was 3.3%, three times more efficient compared to the earlier mentioned simple leaching tests with HCl of 0.9%. When the HCl step was performed at 50°C instead of 20°C, the extraction efficiency even reached 6.9%.

Nonetheless, considering the overall mass balance, the results are not promising enough. Because the extraction percentage is in this case calculated as the calcium extracted from the F2 material present in the second step, it must be observed that only 20-40% of the original diopside formed F2, depending on the separation efficiency of the size classifying equipment.

Magnesium remained rather insoluble during the two-step experiment at 20°C with an extraction efficiency of 0.2%, although the temperature increase to 50°C resulted into an extraction efficiency of 2.3%.

To somewhat simplify the two-step process, NH_4Cl and HCl were added in the same reaction step. Thus, the hydrated particles would be simultaneously contacted with the acid, allowing also the larger diopside particles to react further.

The two developed (rather complex) process schemes with aqueous solutions are shown in Figure 14.

Different concentrations of both NH_4Cl and HCl were tested at 20°C. Experiments showed that the hydration efficiency decreased with the simplified arrangement, but the calcium extraction efficiency varied between 3-5%, now calculated per total mass of diopside instead of mass F2 only. The weaker acid solution (0.15M HCl, pH: 0.74) had an extraction efficiency of 3.4% while for the stronger acid solution (0.5M HCl, pH= 0.3) the extraction of calcium was 4.4%. Magnesium extraction was only 0.8% and 1.5%, respectively.

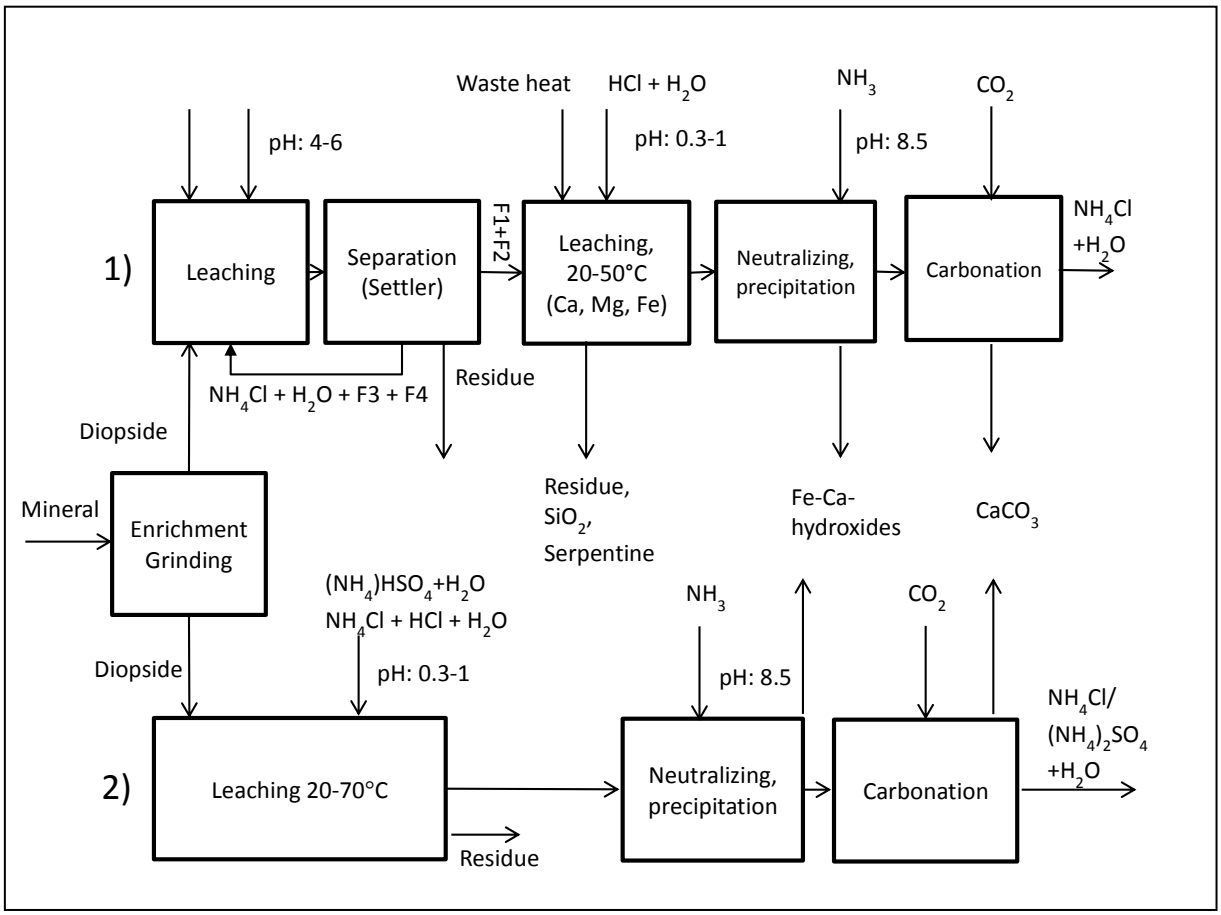

Figure 14. The two developed process options

3.2.6 Indirect carbonation of leached elements

Because the solution pH value is too low for carbonation after the acid leaching step, a pH adjustment is required. For that purpose (aqueous) ammonia is used, forming appropriate salts with the chosen acids. These salts could be recycled in the process. In the ÅA-route (Figure 1) the first precipitation step is performed at a pH of 8-9 to achieve a complete iron precipitation. Fe^{3+} ions precipitate at pH 4, and Fe^{2+} ions at pH 8. Calcium compounds precipitate at pH conditions above 7. The following precipitation step of the ÅA route, precipitation of magnesium hydroxide, would require a pH of 11.0-11.5, (Romão et al., 2015). Because the Mg content and extraction efficiency were very low in the diopside based experiments, the target in this case was to carbonate calcium.

According to SEM/EDS analyses the obtained precipitate contained mostly iron and calcium hydroxides and carbonates, but also traces of silicon and chlorides. The latter originated from ammonium chlorine salt residues, remaining in the filtrate. The SEM/EDS results can be found in Appendix E, and the experimental results are summarized in Table 7. The carbonate content of the precipitate varied between 33

and 96%, calculated as calcium carbonate. The best results using this method of capturing CO_2 were roughly 5 mg/g diopside.

Table 7. Experimental parameters and some obtained results of the indirect carbonate precipitation tests.

Exp.	Steps	Solvent	Temp. (°C)	Diopside (g)	Precipitate at pH 8.5 (g)	$CaCO_3$ (%)
69	2	NH_4Cl / HCl	20	5.2	0.13	96
72	2	$(NH_4)_2SO_4$ / HCl	50	5.5	0.18	90
74	1	0.1 M NH_4Cl / 0.15 M HCl	20	30	0.43	33
75	1	0.1 M NH_4Cl / 0.5M HCl	20	30	0.45	91
78	1	1.4 M NH_4HSO_4	20	20	-	35

3.3 Aqueous Ammonium bisulfate (ABS) experiments

3.3.1 Leaching in ABS solutions

To perform a direct comparison with earlier results (Sanna et al. 2014), also ammonium bisulfate (ABS) was tested as a lixiviant instead of ammonium chloride. Figure 15 shows that only about 6% of Ca and 2% of Mg were extracted using a 1.4M solution of ABS. Calcium and magnesium extraction efficiencies follow a trend seen in Figure 16 and Figure 17, respectively. Solution pH clearly affects the extraction efficiency.

Experiments were performed at 70°C in a stirred aqueous reactor with 0.4l 1.4M ABS solution. The more concentrated, warm aqueous reaction showed improved extraction results with doubled extraction efficiency of 6.7%-wt. for Ca and 2.4%-wt. for Mg. Still, these are low numbers compared to the literature results reported of Mg extraction of 30%-wt. in three hours from the pyroxene-type material, (Sanna et al., 2014).

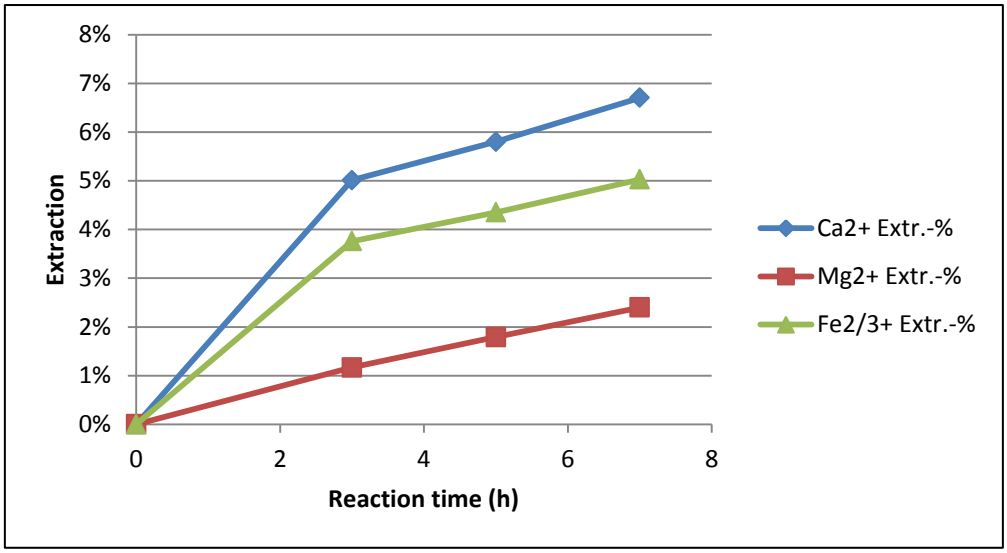

Figure 15. Extraction efficiency of calcium, magnesium and iron with a 0.4l, 1.4M ABS solution at 70°C. The result of experiment 79 is shown.

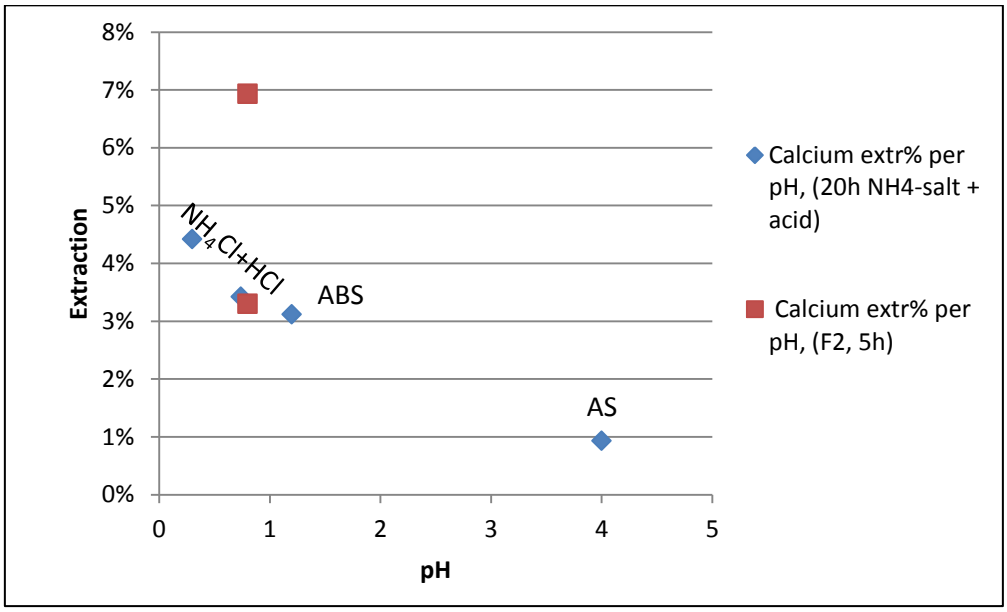

Figure 16. Extraction efficiency of calcium depending on pH. Two-step tests with acid leaching of F2 are colored red. The extraction-% is calculated from the size fractions mass-% shown in Figure 10. Leaching time in all these experiments was five hours. One-step test results are colored blue, and the extraction-% is calculated from entire diopside mass after 20h. The results of experiment 67, 68, 69, 72, 74 and 75 are shown.

The pH value of the solution has an impact on the calcium extraction efficiency from diopside at varying pH. As H^+ concentration increases, extraction efficiency is improved (Figure 16).

A leaching test with 0.1M ammonium sulfate salt with the pH-value 4, confirms that the lower concentrations of H^+ also lower the extraction efficiency under 1%. The extraction was considerably faster and more efficient at higher temperatures.

However, the extraction is still quite inefficient since about 90-95% of the mineral remained insoluble.

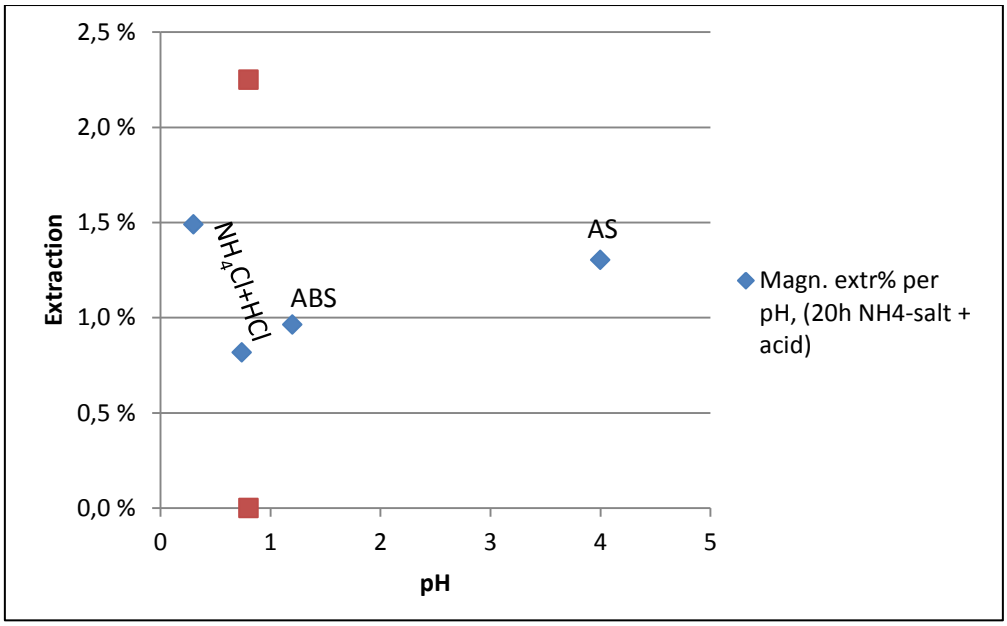

Figure 17. Extraction efficiency of magnesium depending on pH. Two-step tests with acid leaching of F2 are colored red. The extraction-% is calculated from the size fractions mass-% shown in Figure 10. Leaching time in all these experiments was five hours. One-step test results are colored blue, and the extraction-% is calculated from entire diopside mass after 20h. The highest extraction was obtained at 50°C, other tests at 20°C. The results of experiment 67, 68, 69, 72, 74 and 75 are shown.

In the experiments 78, 79 and 83, 20 grams of diopside was added to a 0.4 l, 1.4M ammonium bisulfate solution, according to the procedure of Sanna et al., 2014 (Figure 18). Experiment 83 refers to a test done with burnt diopside. The results show that the experiment with burnt diopside follows the trend of the unburnt diopside. No mineralogical change caused by the treatment was found according to XRD analyses, and the treatment did not affect the leaching process.

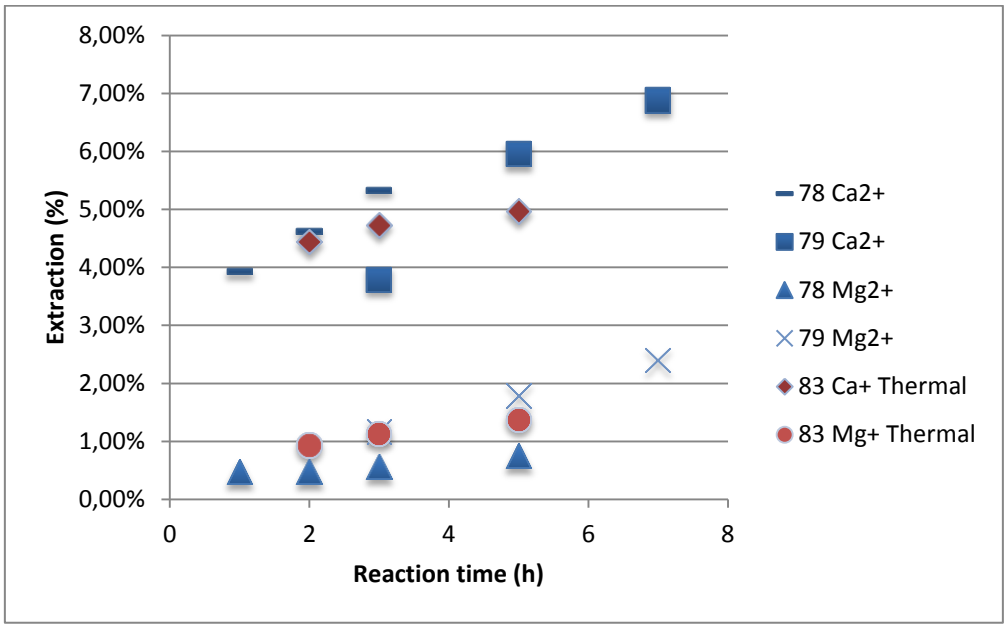

Figure 18. Extraction efficiencies reached by leaching in ABS solutions of Ca and Mg for the unburnt enriched diopside-rich fraction (blue) and the burnt enriched diopside-rich fraction (red). The results of experiment 78, 79 and 83 are shown.

3.4 Thermal solid/solid reaction routes

One alternative approach is to use the concentrated diopside-rich rock directly as an input material in the first step of the ÅA route.

To be able to study the extraction from the rock, it was sufficient to run the thermal solid/solid reaction and dissolve the extracted material in distilled water. The process steps accordingly are shown in Figure 19. The dissolved material was analyzed with AAS and the extraction efficiencies from the rock will be presented in following chapters. An overview of the solid/solid experiments can be found in Appendix F.

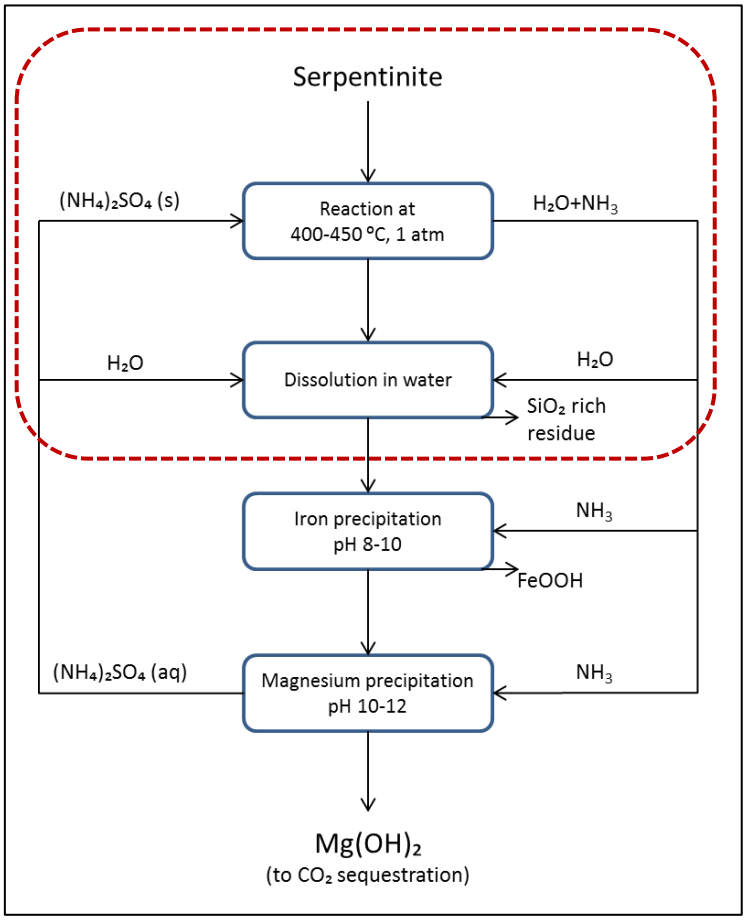

Figure 19. Process scheme of the conventional ÅA route. Extraction efficiency was calculate from AAS analyses of Ca, Mg and Fe in the outgoing solution (from steps marked with red dots).

The tests were done either in a rotary kiln or in a chamber furnace (Figure 20 and Figure 21).

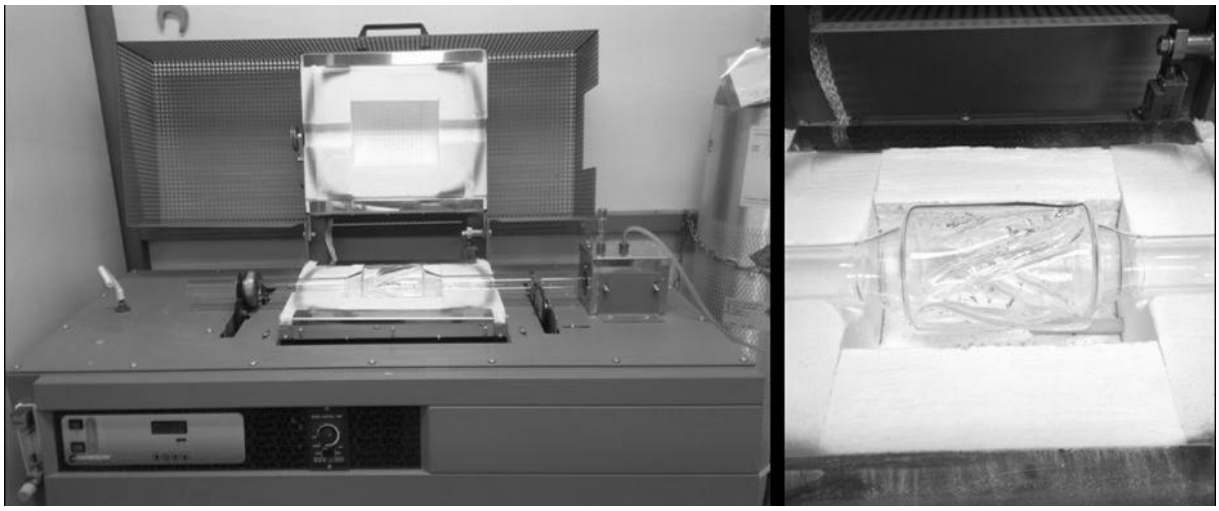

Figure 20. Rotary kiln

Figure 21. Chamber furnace

Table 8 presents a summary of the experiments done with solid/solid reaction options. The method and presentation of the results are presented in following sections. The weight decrease of the material was very low in the thermal solid/solid reaction. The largest weight loss was calculated to 6.8 %-wt. for a test with fraction F2 and ABS, and is calculated based on the total ingoing mass of the rock used.

Already the large amount of insoluble material indicates that the side-rock from the limestone quarry probably would be much less reactive than earlier studies by others, (Sanna et al., 2014, and D513).

Table 8. Experimental parameters for thermal solid/solid reactions either with ammonium sulphate (AS) or ammonium bisulphate (ABS). Tests are run either in a rotary kiln or in a chamber furnace. D= diopside containing rock, B=burnt, UC=unconcentrated, *=chamber furnace (kiln used in all other tests), F2=fraction F2 used as feed instead of diopside based rock. Distilled H_2O (2/15 ml) was added to the material mixture before running the tests for the first three types of tests in the table.

Mineral	Mineral (g)	Reagent	Reagent (g)	Temp (°C)	Time (min)	H_2O (ml)	Ca^{2+} ext.	$Fe^{2/3+}$ ext.	Mg^{2+} ext.	Wt. loss (%)
D, 125-250	40.00	ABS	40.00	90	180	15+500	**4.3**	**4.1**	**3.6**	**-3.0**
D, B, 125-250	30.00	ABS	30.00	90	240	15+375	**2.7**	**1.2**	**1.0**	**-2.7**
*, D, 63-150	25.00	ABS	25.00	440	60	2+315	**4.5**	**1.8**	**1.2**	**0.1**
*, D, 63-150	25.00	ABS	25.00	440	60	315	**4.6**	**2.1**	**1.7**	**-0.2**
D, B, UC, 125-250	40.00	AS	50.00	440	60	500	**4.8**	**0.2**	**0.1**	**6.9**
D, UC, 125-250	30.00	ABS	40.00	440	60	375	**6.1**	**0.3**	**0.1**	**2.2**
D, 125-250	40.00	AS	50.00	440	60	500	**3.1**	**0.2**	**0.1**	**-1,1**
*, F2	1.00	ABS	1.00	480	60	40	**6.1**	**2.2**	**1.5**	**-6.8**
*, F2	1.00	AS	1.25	480	60	40	**5.1**	**1.2**	**0.8**	**-5.6**
D, B, 125-250	30.00	ABS	30.00	440	60	375	**1.7**	**0.2**	**0.3**	**-2.3**

The mass of the unconcentrated fractions after the solid/solid reactions increased. An explanation for this could be that calcium oxide, CaO, in the sample will react with the water during dissolution forming $Ca(OH)_2$, which in turn will increase the total weight of insolubles.

3.4.1 Solid/solid reactions with ABS and H_2O

As a modification of the replicated tests done by Sanna et al. (2014), two tests were run in a rotary kiln (Figure 20) for 3 and 4 hours using both un-burnt and burnt concentrated diopside, respectively (Table 8). The amount of water was very small since larger amounts could have caused water to start to flow out of the glass reactor. Extraction of Ca, Fe, and Mg between 1.0 and 4.3 %-wt. was obtained for these experiments. ”Best” extraction of magnesium of 3.6 %-wt. amongst all solid/solid reactions run was achieved from the test run at 90 °C for 3 hours using concentrated, unburnt wall rock.

Another two samples with 25 g of diopside-rich material (63 -125 µm, concentrated) and 25 g of ABS respectively, were prepared. In addition, 2 ml of distilled H_2O was added to one of the samples. A minor amount of water could possibly improve extraction according to earlier studies (Romão et al., 2013). The material mixes were inserted to ceramic crucibles and put in a pre-heated chamber furnace (Figure 21). The mixture was allowed to react at 440 °C in 60 minutes. The material was thereafter removed from the furnace and cooled for approximately 15 minutes in the ventilation chamber. The crucibles were emptied by washing and dissolving the material with 315 ml of distilled H_2O. Insolubles were thereafter filtered. AAS analyses of Ca^{2+} and Mg^{2+} ions in solution showed that extraction of slightly above 1

%-wt. and 4 %-wt. were reached, respectively (Table 8). Water seemed to lower the extraction efficiency slightly, and none of the experiments gave any sufficient extraction of Ca and Mg.

Earlier studies showed that replacement of ammonium sulfate with ammonium bisulfate, might give better extraction, (Romaõ et al, 2013). Recirculation, however, becomes an issue since ABS will decompose to AS upon heating which would then require additional treatment steps in order to recover the ABS fed to the process.

3.4.2 **Unconcentrated diopside**

Both burnt and unburnt material were mixed with ABS and run through the first solid/solid reaction step of the ÅA route, followed by dissolution of the reacted material. Extraction efficiency of Ca^{2+} up to 6 %-wt. was reached while Mg^{2+} extraction efficiency only reached 0.1 %-wt.

The unconcentrated material was behaving differently from concentrated diopside, since a clear separation of the insoluble material appeared during filtration. Lighter, whitish material was first following the filtrate onto the filter paper and heavier, greyish particles were filtered towards the end. The phases were filtered on separate filter papers and then analyzed with SEM/EDX. Analysis results for a sample with un-concentrated side-rock reacted with ABS are found in Appendix G and H, showing that the lighter insoluble fraction contains more $CaSO_4$ than the following denser insoluble fraction containing higher amounts of the expected SiO_2, which should contribute to the insoluble fraction in the conventional ÅA route.

$CaSO_4$ is most likely a result of a reaction with AS/ABS and calcite ($CaCO_3$), which is present to 5-10 wt-% in the unconcentrated rock (Table 2). $CaSO_4$ is slightly soluble in water. Some of the $CaSO_4$ will therefore remain in the insoluble fraction, especially if the amount of water is too low to be able to dissolve all $CaSO_4$ present.

3.4.3 **Concentrated diopside**

Two samples of fraction ”F2” (section 3.2.2) were mixed with AS and ABS, respectively, in order to see if already processed material could improve the extraction of Mg and Ca ions from the rock by applying the ÅA route (modified in the case where ABS was used). Detailed experimental parameters can be found in Table 8.

An extraction efficiency up to 6 %-wt. of Ca^{2+} from fraction F2 (originating from concentrated diopside) was reached also in this type of test. However, even if extraction were further improved, it should be taken into account that F2 usually is about 10 %-wt. of the ingoing concentrated diopside. The concentrated diopside is in turn about 10 %-wt. of the total rock, which will make the ratio of tonne rock/tonne CO_2 very large (unsuitable).

4 Conclusions

The concentrated diopside fraction studied originating from a limestone quarry wall rock seems to be significantly less reactive than the diopside-containing pyroxene used in literature sources. Best extractions of Mg, Ca and Fe for different types of are presented in Table 9.

Table 9. Summary of best extractions for different types of experiments. Numbers in parentheses refers to a 3 h retention time while the other number in the same type of test is for a retention time of 7 h.

Starting material	Type of test done	Mg extr. %	Ca extr. %	Fe extr. %
Burnt diopside	Thermal solid/solid extraction	0.3	1.7	0.2
Concentrated diopside	Thermal solid/solid extraction	1.4	4.4	1.8
Concentrated diopside	Aqueous leaching	1.5	4.4	1.4
Concentrated diopside	Leaching with ABS	2.4 (3.6)	6.6 (4.3)	2.4 (4.1)
Fraction F2	Thermal solid/solid extraction	1.5	6.1	2.2
Fraction F2	Aqueous leaching	2.3	6.9	0.6

No conversion of diopside to serpentine was achieved in any of the experiments aiming for serpentine (reaction R1). Replacing serpentinite by diopside directly as feed material to the ÅA route did not give any enhanced extraction efficiencies. Thermal treatment did not seem to enhance or affect reactivity, and ABS did not seem to improve extraction either.

The un-concentrated wall rock contains calcite, which could release CO_2 when treated. It also contains high amounts of, for example, aluminum which is unsuitable for mineral carbonation and alkali, which makes it unattractive for the ÅA route. Pre-treatment by means of density separation will in this case be needed. It becomes here important to keep in mind that pre-treatment in a concentrating step will give an energy penalty and that the high density, diopside-rich fraction only contributes to approximately 10 %-wt. of the total amount of the wall rock.

Considering that the experiments presented here produced the most efficient extraction of all experiments done with concentrated diopside, it seems clear that the material is not suitable for a mineral carbonation process according to the ÅA route.

5 References

Arizona State University. 2015. Mantle minerals. http://www.public.asu.edu/~sshim5/images/mantle_minerals.html [Accessed: June 26, 2015]

California Institute of Technology. Division of Geological and Planetary Sciences 2015. *Pyroxenes.* http://minerals.gps.caltech.edu/ge114/Lecture_Topics/Pyroxenes/Index.html [Accessed: June 26, 2015]

Deer, W. A., Howie, R. A., Zussman, J. 1992. *An Introduction to the Rock-Forming Minerals – Chain Silicates* pp. 143-155.

Fagerlund, J., Huldén, S.-G., Södergård, B., Zevenhoven, R. 2010. *Gasometric determination of CO_2 released from carbonate materials.* Journal of Chemical Education 87(12):1372–1376

Frost, B. R. Beard, J. S. 2007. *On Silica Activity and Serpentinization*. Journal of Petrology 48(7): 1351-1368

Koivisto, E. 2013. *Utilization Potential of Iron Oxide By-Product from Serpentinite Carbonation.* M.Sc. Thesis. Luleå University of Technology. Luleå, Sweden.

Lu, H-Y., Lin C-K., Lin, W., Liou, T-S., Chen, W-F., Chang, P-Y. 2011. *A natural analogue for CO_2 mineral sequestration in Miocene basalt in the Kuanhsi-Chutung area, Northwestern Taiwan*. Int. J. of Greenhouse Gas Control 5:1329-1338

Metafysica, http://www.metafysica.nl/turing/preparation_3dim_4.html [Accessed: June 17, 2015]

Nduagu, E., Björklöf T., Fagerlund, J., Wärnå, J., Geerlings, H., Zevenhoven, R. 2012. *Production of magnesium hydroxide from magnesium silicate for the purpose of CO_2 mineralization - Part 1: Application to Finnish serpentinite*. Mineral Engineering 30:75-87

Peck, J.A., Farnan I., Stebbins J. F. 1988. *Disordering and the progress of hydration at the surface of diopside: A cross-polarisation MAS-NMR study*. Geochimica et Cosmochimica Acta 52:3017-3012

Romão, I., Nduagu, E., Fagerlund, J., Gando-Ferreira, L. M., Zevenhoven, R. *2012. CO_2 fixation using magnesium silicate minerals. Part 2: Energy efficiency and integration with iron-and steelmaking. Energy 41(1):203–211*

Romão, I. S., Gando-Ferreira, L. M., Zevenhoven, R. 2013. *Combined extraction of metals and production of $Mg(OH)_2$ for CO_2 sequestration from nickel mine ore and overburden.* Minerals Engineering 53:167–170

Romão, I., Gando-Ferreira, L. M., Zevenhoven, R. 2015. *Separation and recovery of valuable metals extracted from serpentinite during the production of $Mg(OH)_2$ for CO_2 sequestration.* Minerals Engineering 77:25-33

Sanna, A., Lacinska, A., Styles, M., Maroto-Valer, M., M. 2014. *Silicate rock dissolution by ammonium bisulphate for pH swing mineral CO_2 sequestration*. Fuel Processing Technology 120: 128–135

Sjöblom, S., Eklund, O. 2014. *Suitability of Finnish mine waste (rocks and tailings) for Mineral Carbonation.* PROCEEDINGS OF ECOS 2014 – 27th International Conference on Efficiency, Cost,Optimization, Simulation and Environmental Impact of Energy Systems (ECOS 2014). Turku, Finland, paper 244

Styles, M. T., Sanna, A., Lacinska, A. M., Naden, J., Maroto-Valer, M. 2014. *The variation in composition of ultramafic suitability for carbon dioxide sequestration by mineralization following acid leaching.* Greenhouse gases: Science and technology: 4(4):440-451

Zevenhoven, R., Slotte, M., Åbacka, J., Highfield, J.. 2015*. A comparison of CO2 mineral carbonation processes involving a dry or wet carbonation step.* PROCEEDINGS OF ECOS 2015 – 28th International Conference on Efficiency, Cost,Optimization, Simulation and Environmental Impact of Energy Systems (ECOS 2015). Pau, France, paper 51128

Deliverables CCSP

D510. Slotte, M., Romão, I. S., Zevenhoven, R. 2013. *Design and technical feasibility study of a magnesium silicate carbonation demo-plant at an industrial lime kiln*. Cleen CCSP. WP5.2.

D513. Zevenhoven, R., Nduagu, E., Romão, I. S. 2014. *Investigation of alternative-silicate raw material of carbonation*, Cleen CCSP. WP 5.2.

D527. Said, A., Zappa, W., Eloneva, S. *Report on results obtained with demo unit at Aalto*. Cleen CCSP. WP5.

D528. Hudd, H. 2014. *Post-treatment of precipitated calcium carbonate (PCC) produced from steel converter slag.* M.Sc. Thesis. Åbo Akademi University. Finland, Turku.

D532. Mattila, H-P., Hudd, H., Zevenhoven, R. 2014. *Studies on the Slag2PCC process at Åbo Akademi University.* Cleen CCSP. WP5.2.1.

Appendices

A. HSC 8.0 equilibrium diagram for diopside decomposition under acidic conditions

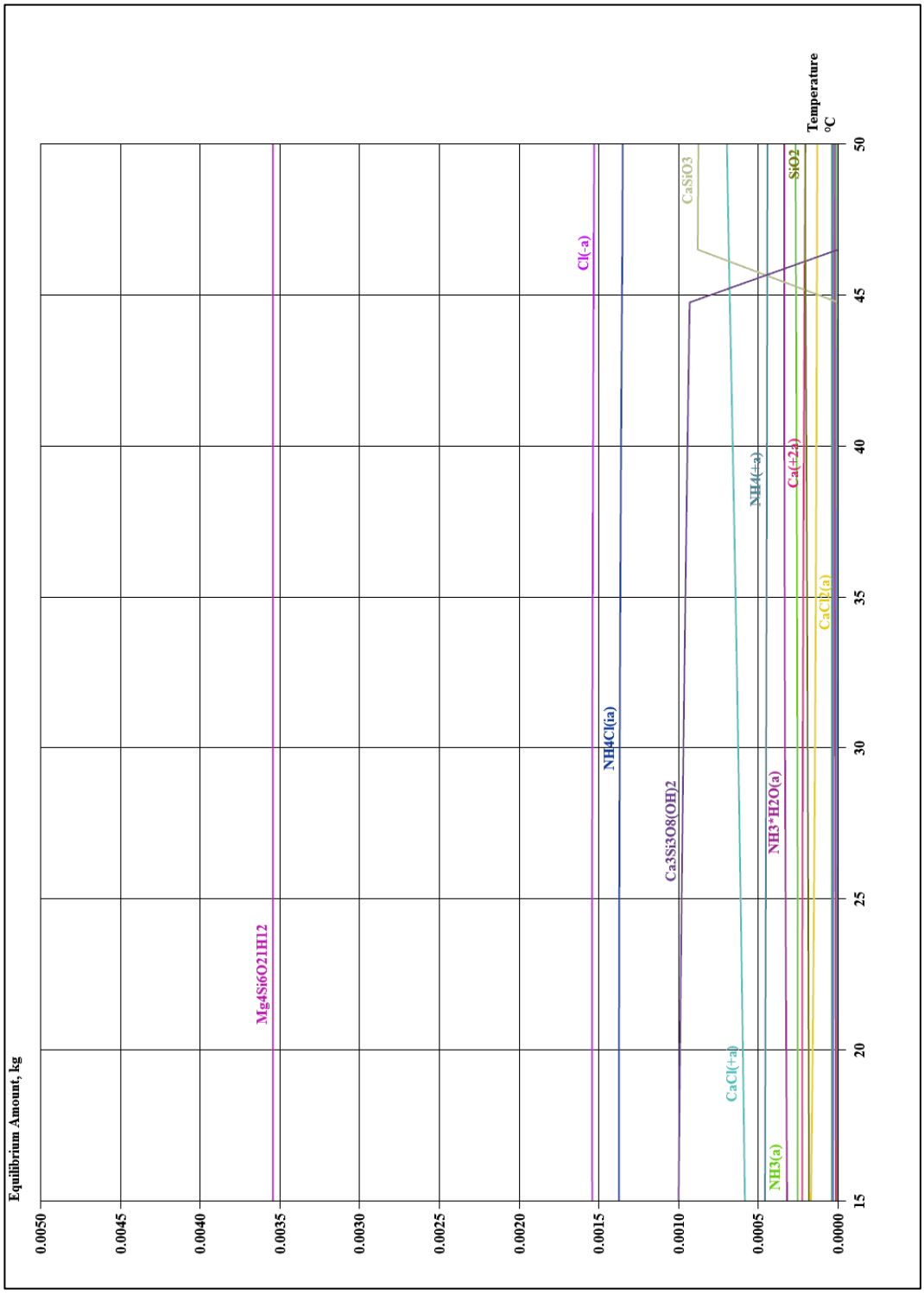

Figure A-1. HSC 8.0 equilibrium diagram for diopside decomposition under acidic conditions.

B. HSC 8.0 equilibrium diagrams for diopside and serpentinite

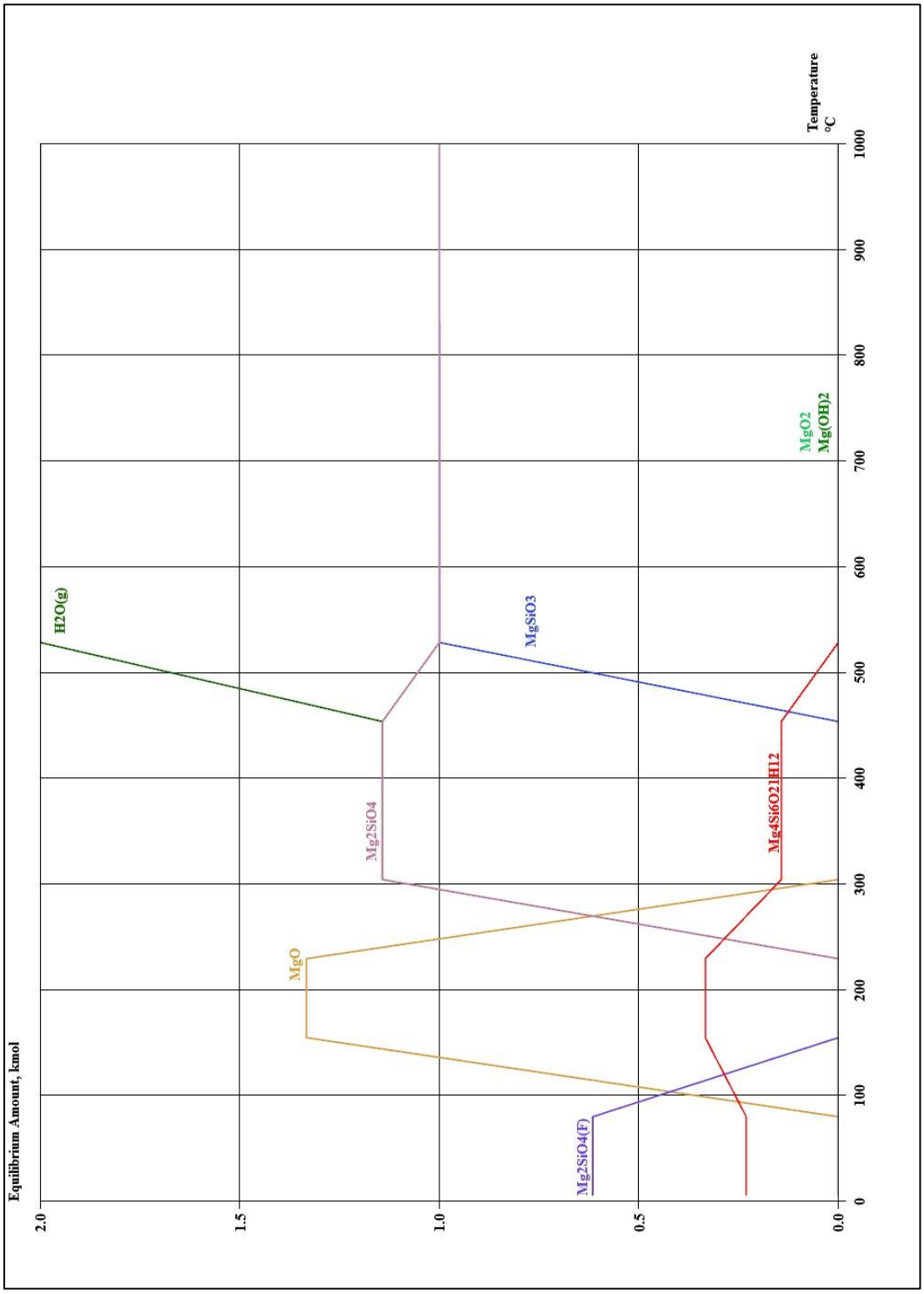

Figure B-1. Equilibrium diagram for serpentinite decomposition at temperatures between 0 and 1000 °C.

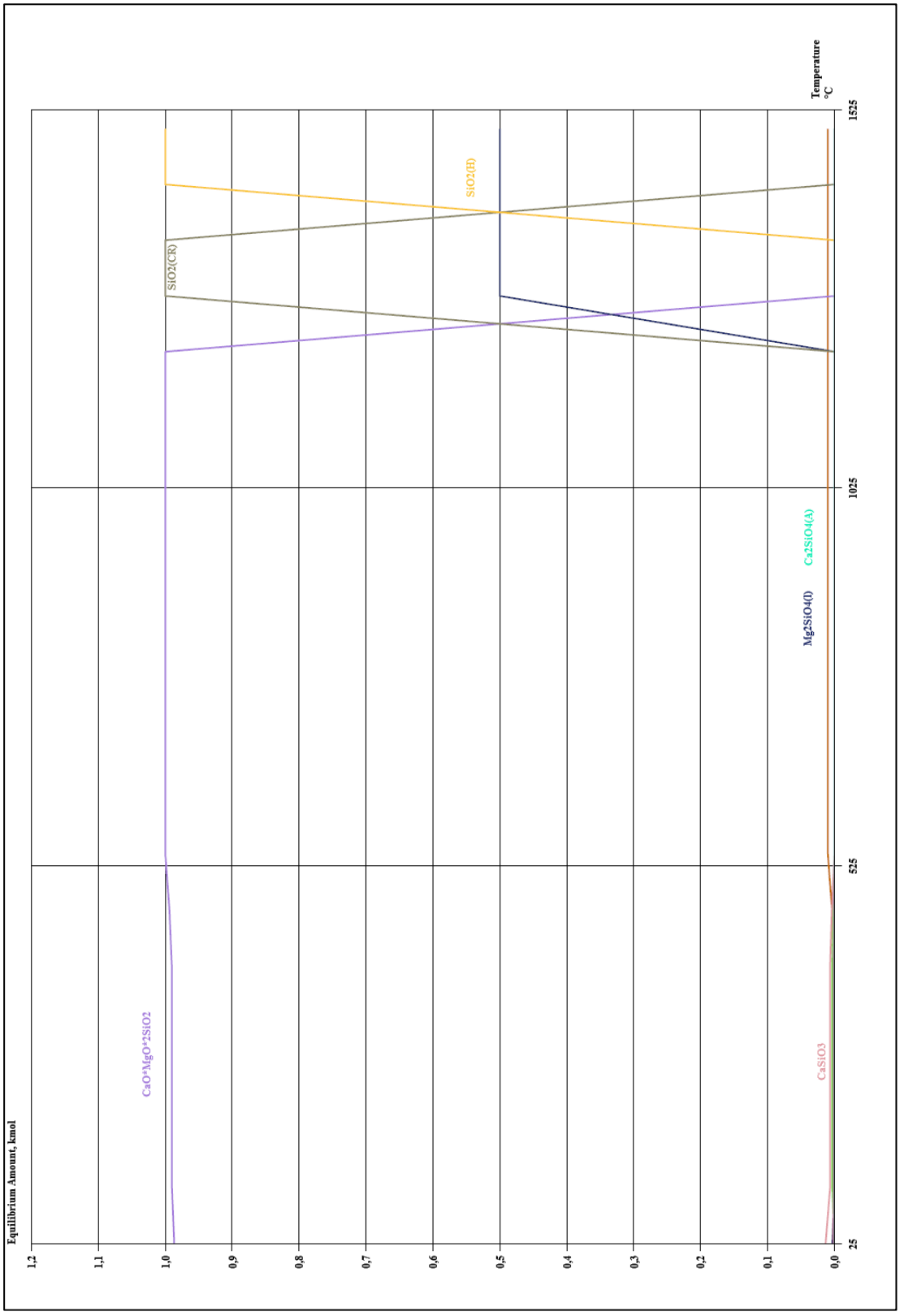

Figure B-2. Equilibrium diagram for diopside decomposition at temperatures between 0 and 1525°C.

C. XRD analyses from experiments 8, 58 and 60

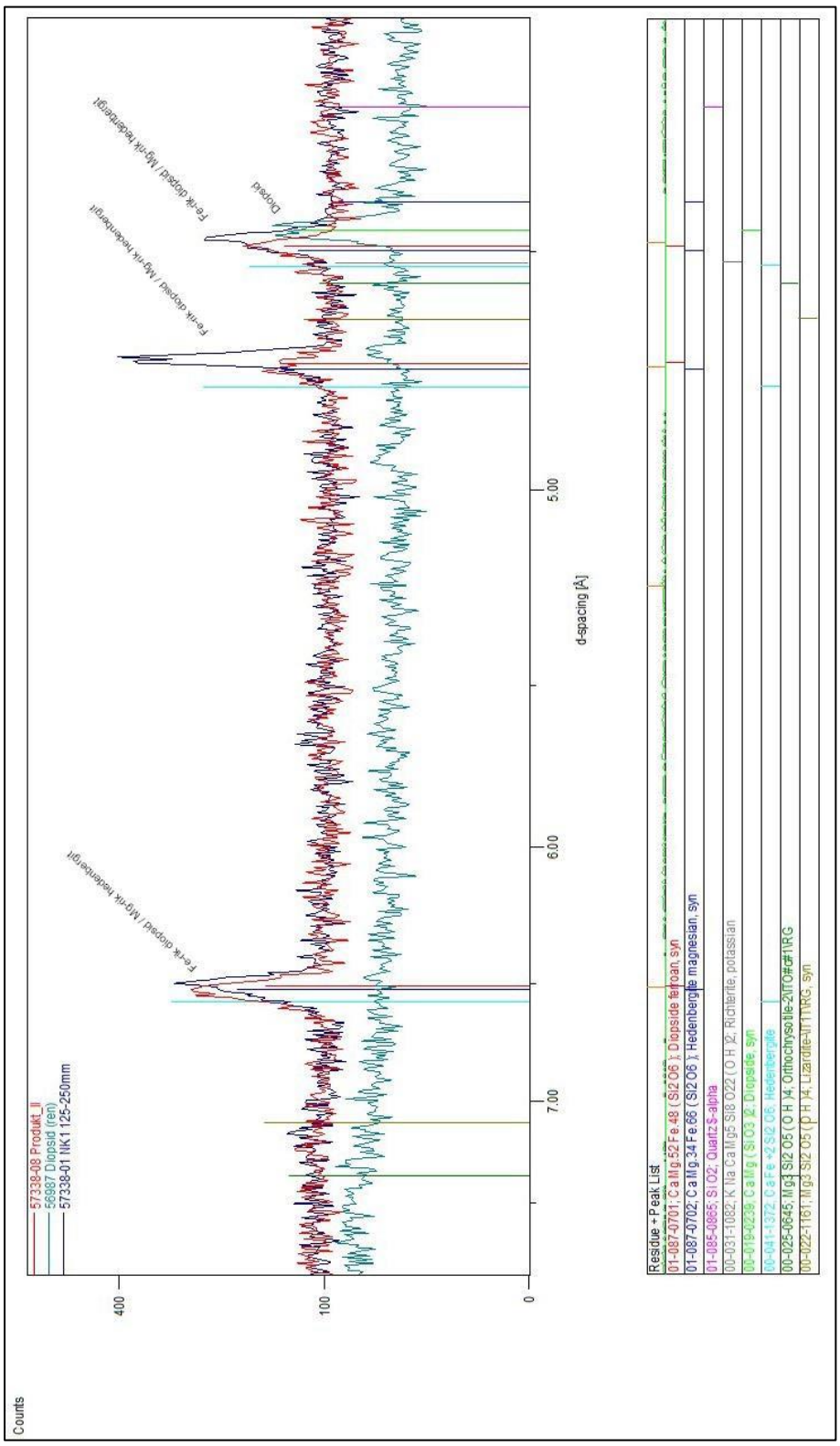

Figure C-1. XRD-analysis of experiment 8. No significant change is recognizable between the start material (blue) and the product (red) in experiment 8. The green line is for pure diopside.

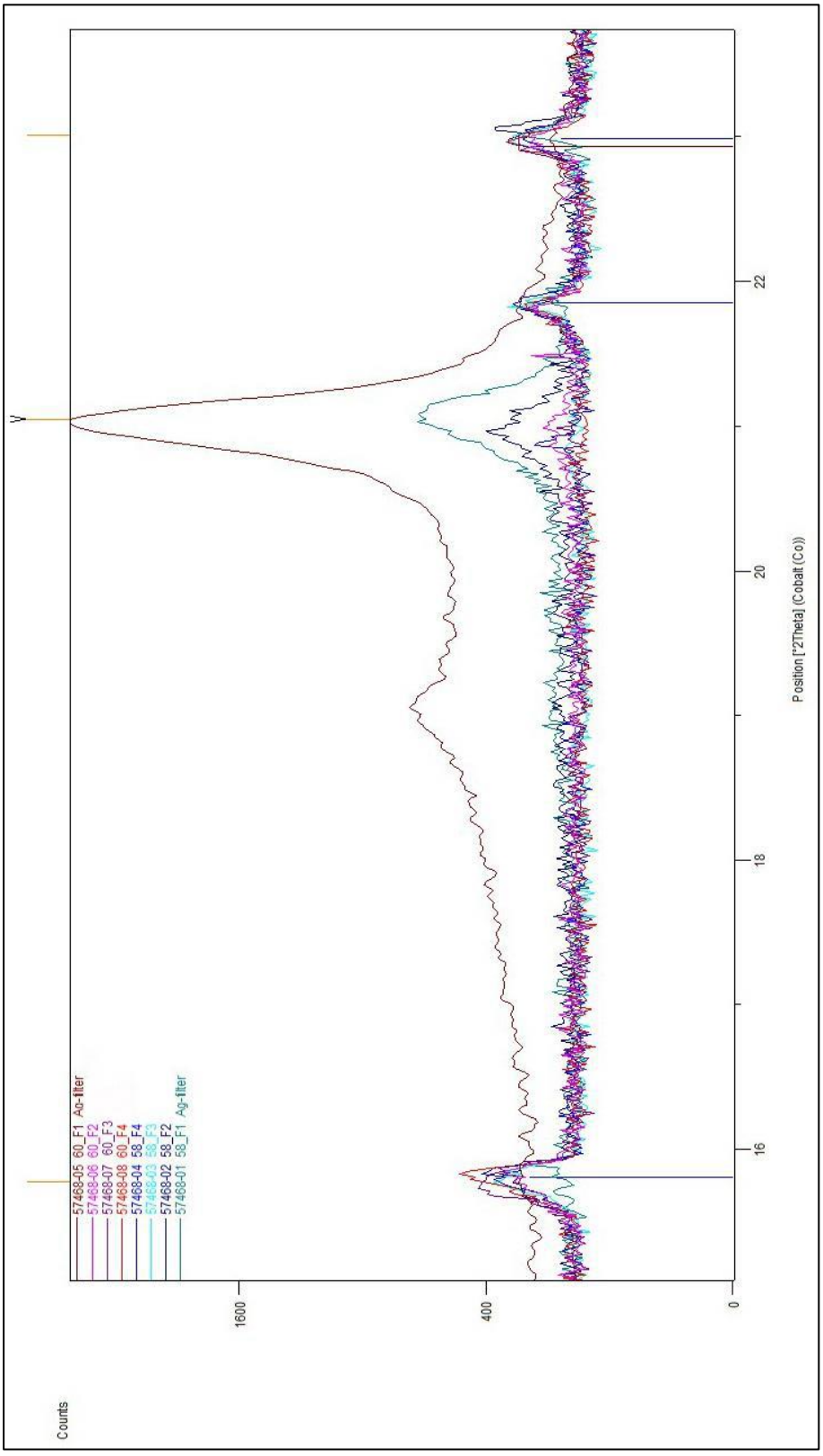

Figure C-2. XRD of experiments 58 and 60. The peak at position 21 shows that only the fractions with small particle size contain $Ca(OH)_2$. The rest of the peaks are similar for the starting material, larger particles and smaller particles, which indicates that no mineralogical changes occurred.

D. XRF and LOI

Table D-1. The loss of ignition (Gl.f. in the figure) and XRF analysis results for the fractions F2, F3 and F4 of the experiments 58 and 60

XRF-ANALYS 57468 Diopsid 58 – 60

Prov		58_F2	58_F3	58_F4	60_F2	60_F3	60_F4
		02	03	04	06	07	08
Element	Enhet						
CaO	%	18.6	21.7	22.6	19.9	22.0	22.6
SiO2	%	42.0	48.6	50.3	47.6	48.8	50.4
TiO2	%	0.77	0.99	0.68	0.86	1.0	0.74
Al2O3	%	2.7	2.5	1.5	2.9	2.5	1.5
Fe2O3	%	14.0	15.9	16.6	14.9	15.7	16.6
MgO	%	6.2	6.9	7.6	6.7	7.1	7.6
K2O	%	0.27	0.24	0.07	0.28	0.21	0.06
Na2O	%	0.45	0.28	0.22	0.50	0.44	0.20
MnO	%	0.23	0.27	0.29	0.27	0.26	0.26
P2O5	%	0.13	0.08	0.05	0.13	0.09	0.06
F	%	<0.01	<0.01	<0.01	<0.01	<0.01	<0.01
Cl	%	<0.01	0.03	<0.01	<0.01	0.06	0.04
S-XRF	%	<0.01	<0.01	0.02	0.02	0.02	0.02
Gl.f 550°C	%	13.9	2.3	0.12	5.4	1.6	0.11
Gl.f 550-1000°C		0.52	-0.05	-0.46	0.29	-0.01	-0.43
Gl.f 110-1000°C	%	14.3	2.3	-0.34	5.7	1.6	-0.32

XRF-analysen gjordes på 1000°C glödgade prov.

E. SEM + EDS analysis

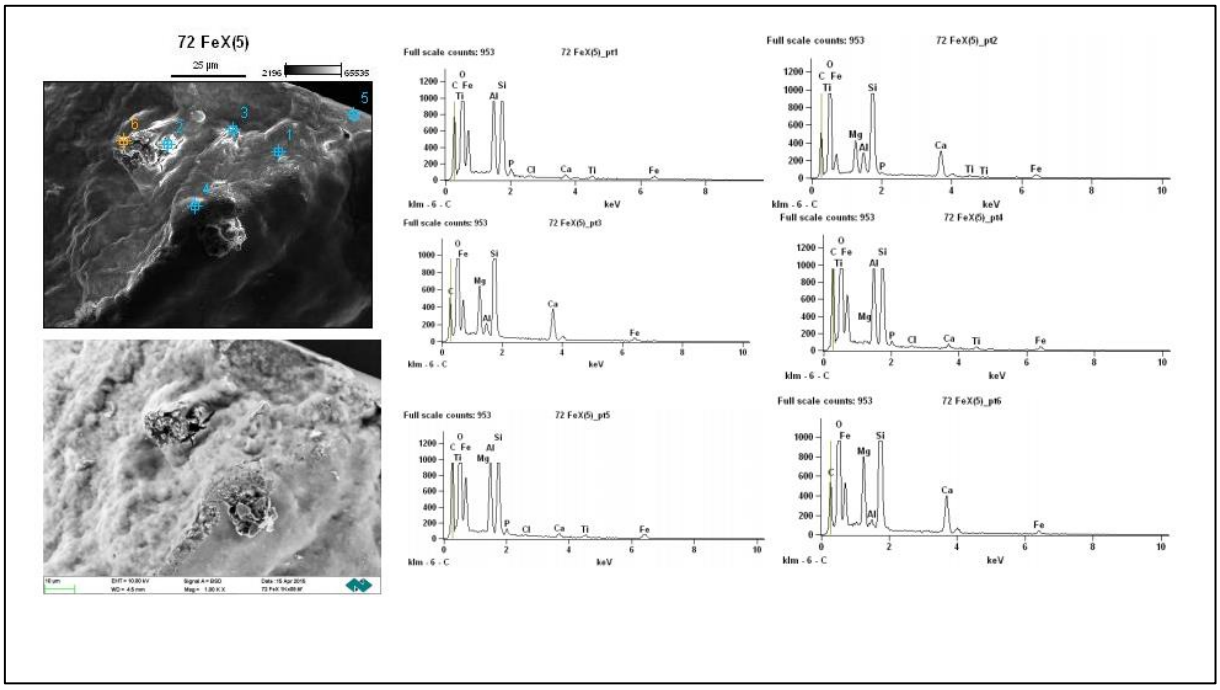

Figure E-1. SEM-EDS analysis of the precipitate at pH 8.5 of experiment 72.

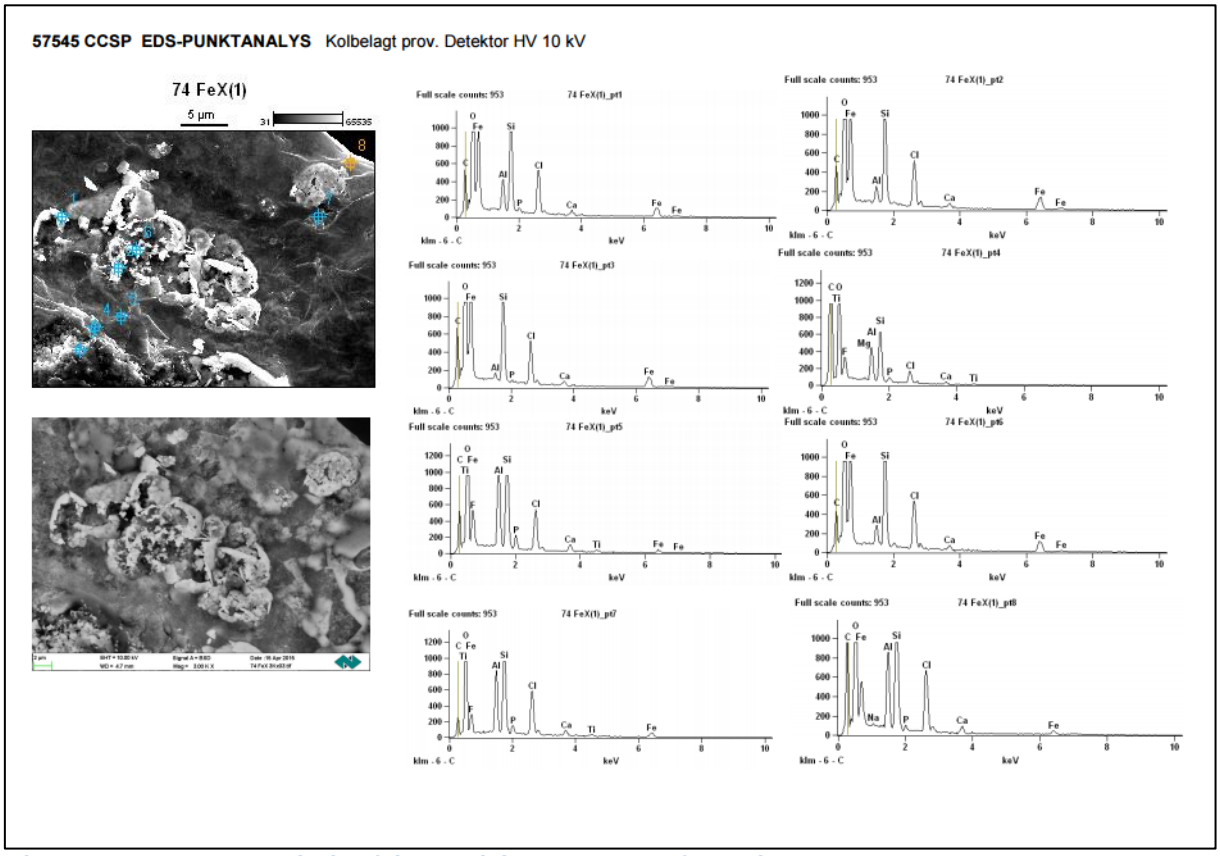

Figure E-2. SEM-EDS analysis of the precipitate at pH 8.5 of experiment 74.

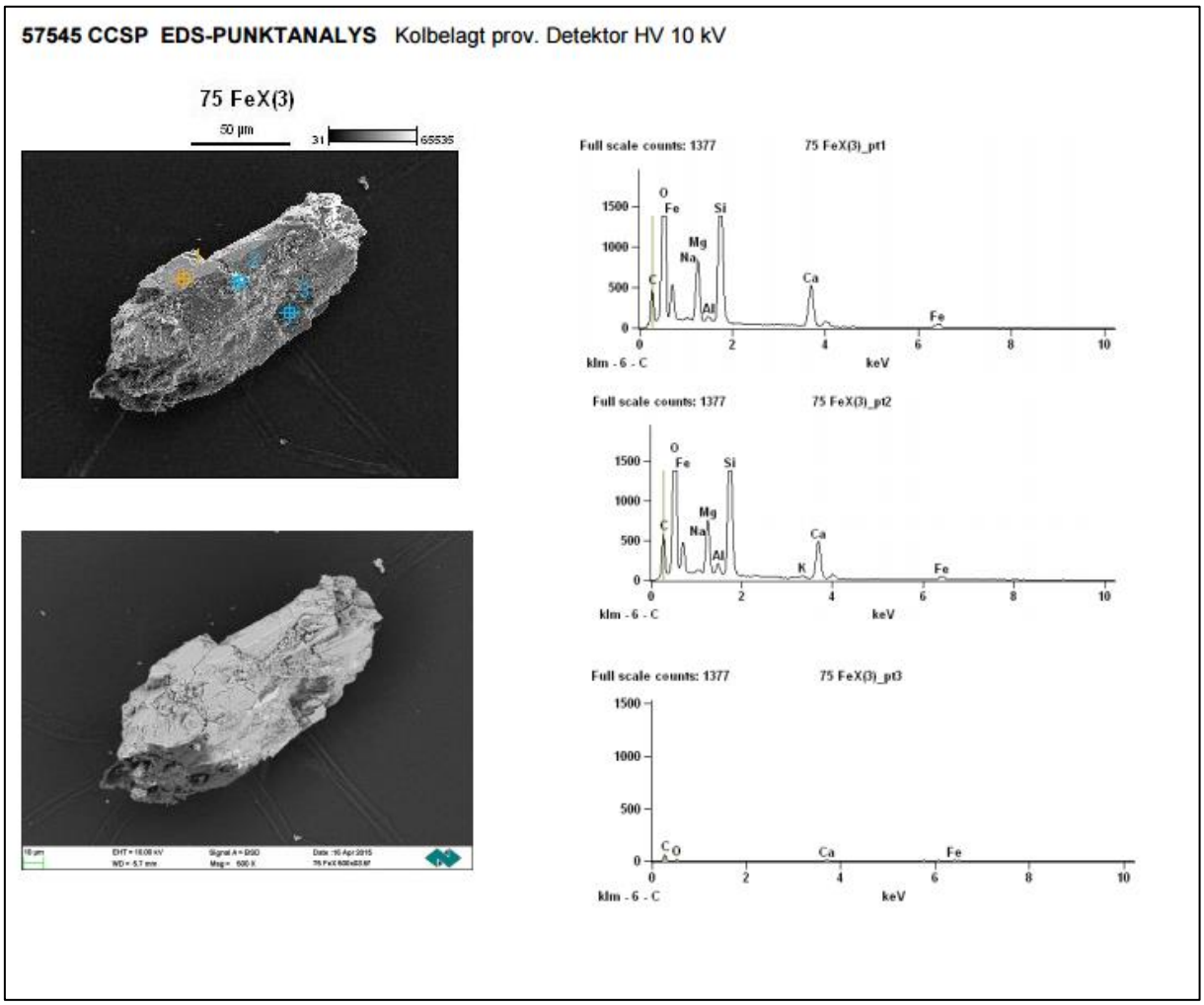

Figure E-3. SEM-EDS analysis of the precipitate at pH 8.5 of experiment 75.

The figures for 72, 74 and 75 FeX can be found in "analysrapport 20.4 2015 57545"

F. Experimental parameters and results from thermal solid/solid reactions

Table F-1. Overview of experimental parameters for thermal solid/solid experiments

Sample Code	Date	Mineral	Mineral (g)	Reagent	Reagent (g)	Furnace	Temp (°C)	Time (min)	Cooling procedure	Dilution (ml)	Insol (g)	% loss	Fe fract (g)	Mg fract (g)
AS	13-16.03.15	Diopside 125-250	40.00	AS	50.00	Rotary	440	60	Rotating until 90C	30 (to kiln) + 470	39.552	-1.1 %	0.485	0.043
ABS-W-65	18.03.15	Diopside 63-150	25.00	ABS	25.00	Chamber	440	60	Cooling in vent chamber	315+2	25.030	0.1 %	0.653	0.038
ABS-D-65	18.03.15	Diopside 63-150	25.00	ABS	25.00	Chamber	440	60	Cooling in vent chamber	315	24.947	-0.2 %	0.613	0.033
ABS-90/3	09.04.15	Diopside 125-250	40.00	ABS	40.00	Rotary	90	180	No cooling needed	15 (in reaction) + 500	38.67	-3 %	-	-
ABS-F2-2	21.04.15	Fraction 2 (no 73)	1.00	ABS	1.00	Chamber (cigar)	480	60	Cooling in vent chamber	40	0.932	-6.8%	-	-
AS-F2-2	21.04.15	Fraction 2 (no 73)	1.00	AS	1.25	Chamber (cigar)	480	60	Cooling in vent chamber	40	0.944	-5.6%	-	-
AS-DI-AB	27.04.15	Burnt, Un-conc diops, 125-250	40.00	AS	50.00	Rotary	440	60	Cooling in glass tube	30 (to kiln) + 470	42.75	6.9%	-	-
ABS-DB-90/4	28.4.2015	Burnt, diopside, 125-250	30.00	ABS	30.00	Rotary	90	240	No cooling needed	15 (in reaction) +375	29.18	-2.7%	-	-
ABS-DB	29.4.2015	Burnt, diopside, 125-250	30.00	ABS	30.00	Rotary	440	60	Cooling in (sealed) glass tube	15 (to kiln) +360	29.3	-2.3%	-	-
ABS-DI-A	30.4.2015	Un-conc, diops, 125-250	30.00	ABS	40.00	Rotary	440	60	Cooling in (sealed) glass tube	15 (to kiln) +360	30.66	2.2%	-	-

Table F-2. Summary of extractions of Ca, Fe, Mg after solid/solid reactions

	Date	13.3.2015	18.3.2015	18.3.2015	25.3.2015	25.3.2015	9.4.2015	21.4.2015	21.4.2015	27.4.2015	28.4.2015	29.4.2015	30.4.2015
Weight tot mineral in (g)		40	25	25	0.85	1	40	1	1	40	30	30	30
H2O tot (l)		0.5	0.315	0.315	0.03	0.03	0.515	0.04	0.04	0.5	0.39	0.375	0.375
Sample name		**AS1**	**W1**	**D1**	**AS-F2-1**	**ABS-F2-1**	**ABS-90/3**	**AS-F2-2**	**ABS-F2-2**	**AS-DI-AB**	**ABS-DB-90/4**	**ABS-DB**	**ABS-DI-A**
Sample number		**01**	**04**	**07**	**01**	**04**	**07**	**01**	**02**				
Element	**Enhet**												
Ca	**mg/l**	**419.7**	**576.8**	**589.0**	**-**	**371.3**	**560.3**	**195.6**	**233.9**	**462.8**	**349.5**	**230.7**	**589.1**
Fe	**mg/l**	**16.1**	**145.6**	**169.8**	**-**	**96.7**	**372.9**	**33.3**	**62.8**	**4.8**	**104.7**	**17.8**	**8.2**
Mg	**mg/l**	**2.9**	**37.5**	**52.7**	**25.5**	**39.4**	**129.6**	**9.1**	**17.5**	**0.81**	**34.5**	**9.3**	**1.2**
Ca	**mg**	209.9	181.7	185.5	-	11.1	288.6	7.8	9.4	231.4	136.3	86.5	220.9
Fe	**mg**	8.0	45.9	53.5	-	2.9	192.0	1.3	2.5	2.4	40.8	6.7	3.1
Mg	**mg**	1.4	11.8	16.6	0.77	1.2	66.7	0.4	0.7	0.4	13.4	3.5	0.5
Ca-in	**%**	16.72	16.01	16.01	15.36	15.36	16.72	15.36	15.36	12.14	16.72	16.72	12.14
Fe-in	**%**	11.81	10.35	10.35	11.19	11.19	11.81	11.19	11.19	3.2	11.81	11.81	3.2
Mg-in	**%**	4.6	3.8	3.8	4.4	4.4	4.6	4.4	4.6	1.2	4.6	4.6	1.2
Ca-in	**mg**	6688	4002.5	4002.5	131	154	6688	154	154	4856	5016	5016	3642
Fe-in	**mg**	4724	2588	2588	95	112	4724	112	112	1280	3543	3543	960
Mg-in	**mg**	1840	950	950	37	44	1840	44	46	480	1380	1380	360
Ca-extract	**%**	**3.1**	**4.5**	**4.6**	**-**	**7.3**	**4.3**	**5.1**	**6.1**	**4.8**	**2.7**	**1.7**	**6.1**
Fe-extract	**%**	**0.2**	**1.8**	**2.1**	**-**	**2.6**	**4.1**	**1.2**	**2.2**	**0.2**	**1.2**	**0.2**	**0.3**
Mg-extract	**%**	**0.1**	**1.2**	**1.7**	**2.0**	**2.7**	**3.6**	**0.8**	**1.5**	**0.1**	**1.0**	**0.3**	**0.1**

G. XRD and XRF analyses on insoluble fractions from tests with un-concentrated diopside or burnt diopside is used

Table G-1. XRF analyses on insoluble fractions from tests with unconcentrated diopside and with burnt diopside

XRF-ANALYS 57617 CCSP, E. Koivisto

	Provnamn Provnummer	AS-DI-AB 05	ABS-DB-90/4 06	ABS-DB 07	ABS-DI-A-1 08	ABS-DI-A-2 09
Element	Enhet					
CaO	%	15.04	21.79	21.37	30.50	13.60
SiO2	%	51.41	49.65	50.00	11.61	55.19
TiO2	%	0.20	0.44	0.34	0.16	0.19
Al2O3	%	13.92	1.59	1.89	3.92	16.10
Fe2O3	%	4.69	17.65	17.14	0.66	4.78
MgO	%	1.98	7.11	7.40	0.20	2.03
K2O	%	3.43	0.12	0.11	0.50	3.76
Na2O	%	1.55	0.23	0.28	0.29	1.60
MnO	%	0.04	0.31	0.33	<0.01	0.04
P2O5	%	0.03	1.46	1.43	0.06	0.02
S-XRF	%	1.52	0.01	0.02	15.15	0.21
Gl.f 110-550°C	%	1.18	0.14	0.14	7.28*	0.58
Gl.f 110-1000°C	%	3.73	-0.47	-0.47	14.20*	1.90

*= gl.f 40-550°C / 40-1000°C pg.a provet innehåller kristallvatten.

Table G-2. XRD analyses on insoluble fractions from tests with unconcentrated diopside and with burnt diopside

XRD-ANALYS 57617 CCSP, E. Koivisto

	AS-DI-AB	ABS-DB-90/4	ABS-DB	ABS-DI-A-1	ABS-DI-A-2
Fältspat	X	X	X	X	X
Diopsid	X	X	X	X	X
CaSO4	X			X	
Bassanit				X	
Kvarts	X			X	
Wollastonit	X				X
(NH4)3H(SO4)2				X (?)	
Amfibol	X	X	X	X	
Kalcit	X				
Serpentin			X (?)		
Epidot/Zoisit					X

H. SEM/EDX analyses on insoluble material from test with un-concentrated side-rock

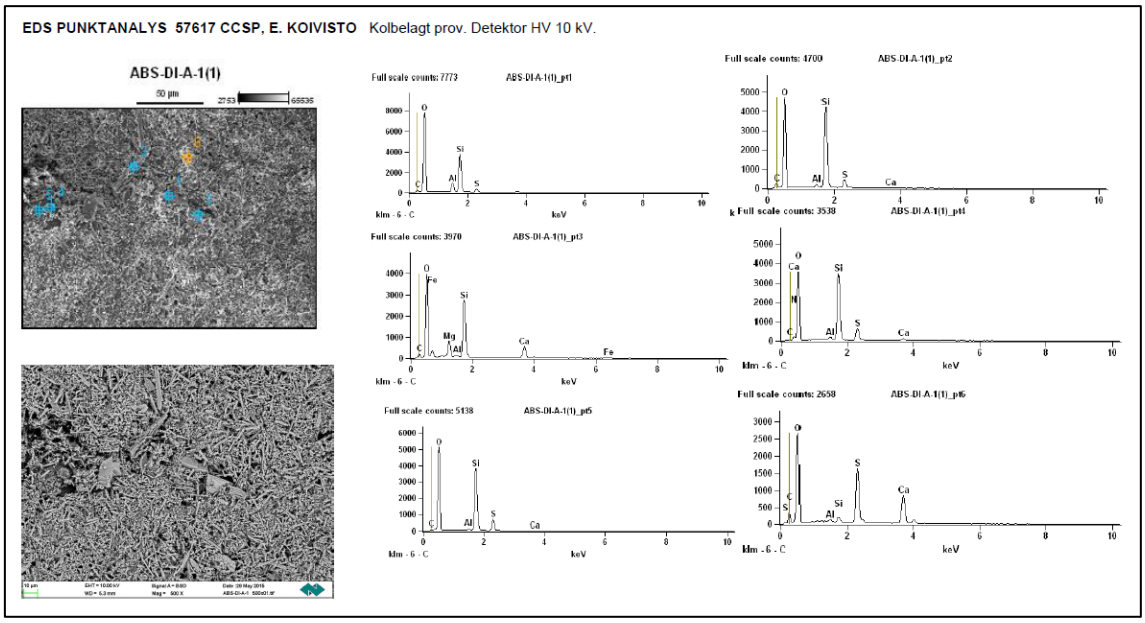

Figure H-1. Insoluble "light fraction" from test ABS-DI-A (see also appendix G code ABS-DI-A-1)

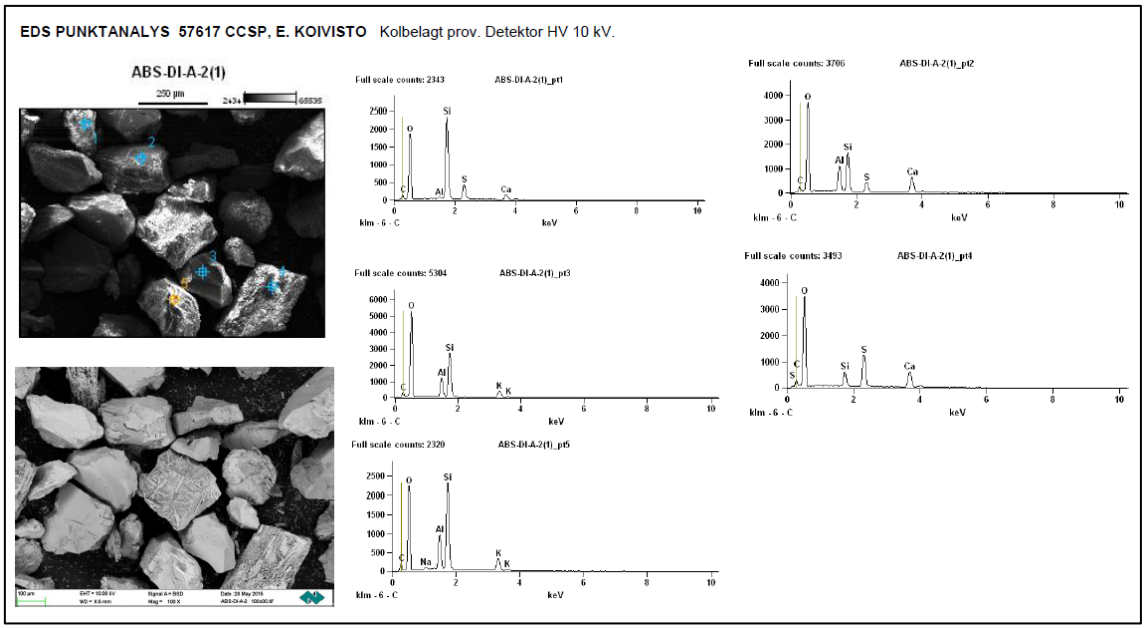

Figure H-2. Insoluble "dense fraction" from test ABS-DI-A (see also appendix G code ABS-DI-A-2)